# SUPPORTING INFORMATION

## Supporting Information

## Boosting PLA melt strength by controlling the chirality of co-monomer incorporation

An Sofie Narmon[a], Annelies Dewaele[a], Kevin Bruyninckx[a], Bert F. Sels[a], Peter Van Puyvelde*[b], Michiel Dusselier*[a]

**Abstract:** Bio-based and degradable polymers such as poly(lactic acid) (PLA), have become prominent. In spite of encouraging features, PLA has a low melt strength and melt elasticity, resulting in processing and application limitations, that diminish its substitution potential vis-a-vis classic plastics. Here, we demonstrate a large increase in zero shear viscosity, melt elasticity, elongational viscosity and melt strength by random co-polymerization of lactide with small amounts, viz. 0.4-10 mol%, of diethylglycolide of opposite chiral nature. These enantiomerically pure monomers can be synthesized using one-step zeolite catalysis. Screening of the ester linkages in the final PLA chains by the ethyl side groups is suggested to create an expanding effect on the polymer coils in molten state by weakening of chain-chain interactions. This effect is suspected to increase the radius of gyration, enabling more chain entanglements and consequently increasing melt strength. A stronger melt could enable access to more cost-competitive and sustainable PLA-based biomaterials with a broader application window

DOI: 10.1039/x0xx00000x

# SUPPORTING INFORMATION

## Table of Contents



## Experimental Procedures

### S1 Materials

(L)- and (D)-α-hydroxybutyric acid (Sigma-Aldrich, ≥97.0%) were used as received. (L,L)- and (D,D)-lactide (Corbion Purac) were purified by recrystallization in toluene (15 ml per 20 g lactide) at 100°C prior to polymerization. Commercial acidic zeolite H-Beta (H-BEA) (Clariant, Si/Al = 12.5 and 75) was used after calcination. Toluene (Acros Organics, 99.5%), o-xylene (Fischer Scientific, 99%), acetonitrile (Acros Organics, ≥99.9%), diethylether (Acros Organics, 99+%), petroleum ether (Acros Organics, boiling range 60-95°C), chloroform (Acros Organics, >99.8%), methanol (Acros Organics, 99.9%), tetrahydrofuran (Biosolve, unstabilized), chloroform-d (Sigma-Aldrich, 100%, 99.96 atom% D, 0.03% (v/v) TMS) and DMSO-d6 (Sigma-Aldrich, 100%, 99.96 atom% D, 0.03% (v/v) TMS ) were used as purchased. Tin(II) 2-ethylhexanoate (Sigma-Aldrich, 92.5-100.0%) was purified and dried by vacuum distillation. n-dodecanol (Sigma-Aldrich, 98.0%) was used as received. Toluene used to dissolve polymerization catalyst and initiator was purified and dried by a MB SPS-800 solvent purification system (MBRAUN).

### S2 Methods

*S2.1 Synthesis and purification of diethylglycolide*

In a typical reaction, 0.01 mol of (L)- or (D)-α-hydroxybutyric acid and 0.5 g of H-Beta zeolite (Si/Al=75) are added to a round bottom flask. Then 20 mL of *o*-xylene and a magnetic stirring bar are added. On top of the round bottom flask, a custom made phase-settler/solvent reflux trap is installed, filled beforehand with o-xylene. This setup is connected to a condenser, and heated in an oil bath at 170 °C. The mixture is stirred for 3 hours. After reaction, the mixture is homogenized by addition of 15 mL of acetonitrile. After homogenization, the zeolite is removed by filtration over a glass frit filter under vacuum. After the first filtration, the catalyst is rinsed with another 10 mL of acetonitrile. 1 mL is taken from the reaction mixture, dried and analyzed by $^{1}$H-NMR.

After reaction and removal of solvents by evaporation under reduced pressure, (L)- or (D)-α-hydroxybutyric acid is separated from the linear oligomers and (L,L)- or (D,D)-ethylglycolide by liquid-liquid extraction in toluene-water (1:1). After collection of the toluene phase and solvent evaporation, a minimal amount of diethyl ether is added to dissolve the product. The solution is cooled at -41 °C in a bath of dry ice in acetonitrile, and petroleum ether is added dropwise until crystallization occurs. Ethylglycolide appears as colorless crystals which

are collected by filtration over a glass frit filter and dried under vacuum. The crystallization procedure is repeated until a purity of ≥ 99.5 % is obtained based on $^{1}$H-NMR.

$^{1}$H NMR (400 MHz, DMSO): 5.31 - 5.26 (2H, t), 2.07 - 1.69 (4H, m), 0.97 (6H, t).
$^{13}$C NMR (400 MHz, DMSO): 168.29, 76.49, 22.95, 9.18.

### *S2.2 Ring-opening polymerization*

Solvent-free ring-opening polymerizations (ROP) is carried out in sealed, custom-made round-bottom flasks dried at 160 °C. In a typical experiment, a desired amount of monomer is added to the flask in an oxygen- and moisture free environment. A solution of stannous octoate in toluene as catalyst (monomer:catalyst = 2500:1) and n-dodecanol as initiator (70 mol% of the catalyst) are added to the monomer. The solvent is removed in vacuo, and the flask is immersed in an oil bath at 170 °C for 70 minutes. After polymerization, the flask is cooled, and the polymer is dissolved in chloroform. A sample is taken, dried under nitrogen flow and analyzed by NMR to determine monomer conversion. The synthesized polymers are separated from the remaining monomers and oligomers via precipitation in methanol, filtered, and dried under reduced pressure.

### *S2.3 Cyclic ester and polymer characterization*

**$^{1}$H and $^{13}$C-NMR** spectra are recorded in DMSO-$d_6$ (Sigma-Aldrich) or $CDCl_3$ (Sigma-Aldrich) on a Bruker Avance 400 MHz spectrometer with a BBI 5 mm probe.

**Gel permeation chromatography** (GPC) is performed using a Shimadzu LC-10AD chromatograph liquid pump and CTO-10A column oven and a RID-10A refractive index detector. Separation is performed on an Agilent D-kolom 5 µm (mixed) with a 1 mL min$^{-1}$ flow of THF at 40 °C. Polystyrene standards are used for calibration. The Mw of the samples is corrected with Mark-Houwink's constants for PLLA (L-PLA) [1].

**Chiral gas chromatography** (c-GC) is used to determine the stereochemistry of the cyclic ester monomers, separating L,L; D,D and L,D enantiomers. Separation is performed on a Hewlet Packard 6890 with a chiral 25 m Agilent WCOT fused silica CP-Chirasil-DEX CB capillary column. The column has an internal diameter of 0.32 mm and a film thickness of 0.25 µm and is equipped with an FID detector held at 350°C. The temperature of the injection port was set at 220°C. The initial column temperature is kept at 50°C for 2 minutes and is subsequently ramped to 200°C at a heating rate of 15°C min$^{-1}$ and held at this temperature for 3 minutes.

**Thermogravimetric analysis** (TGA) is performed on the polymer powders, heating them from 0 to 400 °C at a rate of 10 °C min$^{-1}$ under $N_2$ or $O_2$ atmosphere using a TGA Q500 (TA Instruments).

Method Log:
1: Select Gas: 1 or 2
2: Data storage: On
3: Ramp 10.00°C/min to 400.00°C
4: Isothermal for 1.00 min
5: End of method

**Differential scanning calorimetry** (DSC) experiments are performed with a DSC Q2000 (TA Instruments) by cycling between 0 and 220 °C at heating/cooling rates of 10 °C min$^{-1}$ under $N_2$ atmosphere:

Method Log:
1: External event: On
2: Equilibrate at 0.00°C
3: Ramp 10.00°C/min to 220.00°C
4: Mark end of cycle 1
5: Ramp 10.00°C/min to 0.00°C
6: Mark end of cycle 2
7: Ramp 10.00°C/min to 220.00°C
8: Mark end of cycle 3
9: Ramp 10.00°C/min to 40.00°C
10: End of method

# SUPPORTING INFORMATION

**X-Ray Powder Diffraction (PXRD):** X-ray diffractograms of the polymer materials were obtained by X-ray powder diffraction on a high-throughput STOE STADI P Combi diffractometer in the transmission mode with focusing Ge(111) monochromatic X-ray inlet beams (λ = 1.5406 Å, Cu Kα source).

*S2.4 Rheometry*

Rheological measurements are performed on a strain-controlled Rheometrics ARES (TA Instruments) rotational rheometer.

**S2.4.1 Small Amplitude Oscillatory Shear**

Small amplitude oscillatory shear (SAOS) measurements are carried out using a parallel plate set-up (8 mm diameter) on an AresMelts rheometer, surrounded with a convection oven, purged with N2 gas to minimize polymer degradation during testing. Prior to rheology measurements, polymer samples are compression molded with a Colline Presse 200 E plate press at a temperature of Tm+10°C and a pressure of 50 bar into discs of 8 mm diameter and a thickness of 1 mm. After plate pressing, the polymer discs are vacuum dried overnight at 80°C and subsequently measured.

First, dynamic time sweep measurements are performed to verify the thermal stability of the polymer samples under the applied test-method. The changes in loss- and storage modulus are determined in time at an angular frequency of 10 rad s-1, a strain amplitude of 1 % and a temperature of 185°C during 300 s. Secondly, strain sweep tests are performed by varying the strain amplitude between 0.1 and 10 % to determine the linear viscoelastic regime of the polymer materials. Frequency sweep measurements are carried out at 185 °C with dynamic frequencies ranging from 0.1 to 100 rad s-1 at a strain amplitude of 1-10 %. Consecutively, rate sweep tests are performed applying shear rates between 0.01 and 1 s-1. At each shear rate a waiting time of 30 s is installed to guarantee steady state, while a measuring time of 10 s is applied.

**S2.4.2 Extensional Viscosity Fixture**

Extensional flow properties of the polymers are determined using an Extensional Viscosity Fixture (EVF) set-up on an AresMelts rheometer. Extensional viscosities are measured in strain-controlled stretch experiments with a Hencky strain of 3.4 at 185°C under a $N_2$ atmosphere. The polymer samples are compression molded into rectangular plates of 18.0 mm long, 10.0 mm (± 0.10 mm) wide and 0.80 (± 0.05 mm) thick at a temperature of Tm+10 °C. Prior to stretch measurements the plates are dried at 80°C overnight. The experimental protocol consists of three steps. During the first step a pre-stretch with a stretch rate of 0.0075 $s^{-1}$ is performed on the polymers to compensate for thermal expansion during heating. Before pre-stretch a delay time of 50.0 s is applied to ensure the polymer samples are completely molten. The pre-stretch is followed by a relaxation step of 5.0 s to remove residual stress in the sample before the actual stretch measurement is performed. Finally, the stretch measurement takes place at a constant Hencky strain rate.

**S2.4.3 Haul-off**

To determine the extensional properties of the polymer melts a Göttfert 2002 capillary rheometer is used in combination with a Haul-off apparatus. The polymer material is added to the barrel of the capillary rheometer at 185°C. To create molten polymer strands, the melt is pushed out of the barrel by a piston with a diameter of 12 mm through a die of 2 mm at a piston speed of 0.05 mm $s^{-1}$. The molten strands are attached to the Haul-off apparatus which spins up the molten strands on a wheel, rotating at a pull-off speed of 100 mm $s^{-1}$. The speed is linearly increased at an acceleration of 0.12 mm $s^{-1}$ till the polymer melt breaks.

## Results and Discussion

## S3 Catalytic cyclic ester synthesis

To verify the applicability of the one-step zeolite procedure for the synthesis of other symmetric cyclic ester dimers in addition to lactide (LD) from lactic acid (LA) (R=$CH_3$), α-hydroxy acids with a different R-chain on the α-carbon were screened: glycolic acid (GA) (R=$H_2$), yielding the cyclic dimer glycolide (G), α-hydroxybutyric acid (α-HBA) (R=$CH_2CH_3$), yielding diethylglycolide (EG) and α-hydroxyisobutyric acid (α-HIBA) ($R_1$=$R_2$=$CH_3$), converting to tetramethylglycolide (TMG). In addition, asymmetric cyclic esters were synthesized via co-condensation of lactic acid and α-hydroxybutyric acid partly resulting in methylethylglycolide. Analyses were done according to Dusselier *et al.* [2] and the methods and materials used can be consulted above.

# SUPPORTING INFORMATION

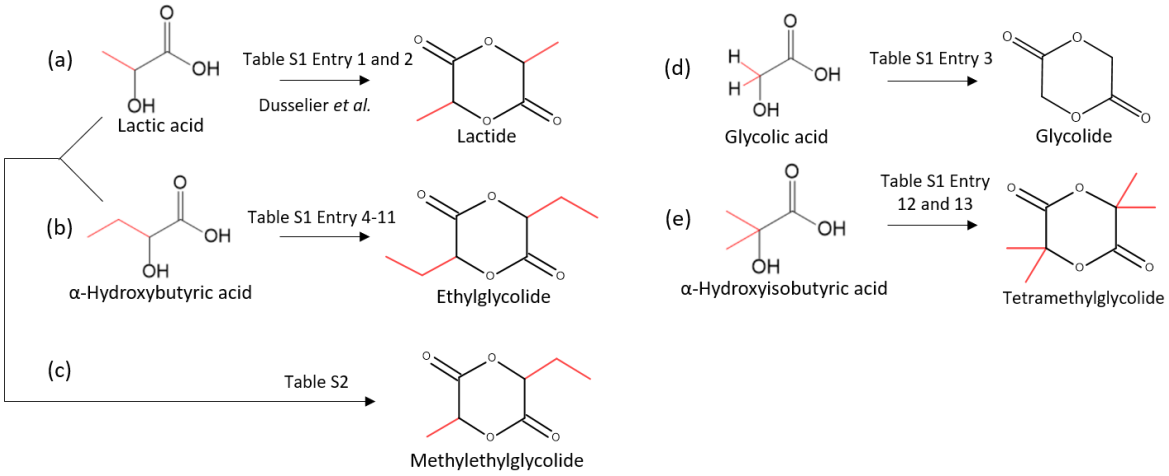


**Fig. S1** Representation of all examined cyclic ester synthesis reactions.

The studied reaction conditions, the final α-hydroxy acid conversion and the cyclic ester yields of the symmetric cyclic esters are represented in Table S1. The conversion of L-LA to (L,L)-lactide (L-LD) in the presence of the Brønsted acidic zeolite Beta ($SiO_2/Al_2O_3$= 25) (H-BEA 25) was used as a benchmark (Table S1, entry 1) [2]. Applying the same conditions to a reaction with GA gave only 4% of G at full conversion (entry 3), compared to 78% of L-LD. Under these reaction conditions, linear oligomerization is favored over ring closure.

Similar cyclic ester yields were attained with L-α-hydroxybutyric acid (L-α-HBA) (entry 5), i.e. 5% (L,L)-ethylglycolide (L-EG), but conversions were low and barely outperforming the blank reaction (entry 4). The meagre reaction outcome at 130°C in toluene indicates a lower reactivity of L-α-HBA than L-LA, suggesting the need for higher reaction temperatures and thus higher-boiling point solvents. These findings were confirmed by using ethylbenzene (entry 6) and o-xylene (entry 7), increasing substrate conversion and L-EG yields up to 76%. Besides the reaction temperature, the type of H-BEA catalyst shows some impact. In the presence of H-BEA ($SiO_2/Al_2O_3$=150), the reaction proceeds both faster and more selective towards the cyclic dimer (88%) (entry 8). As it was already proven in LA reactions with H-BEA (25) that ring closure to LD determines the reaction rate [2], it is unlikely that the improved reaction efficiency of L-α-HBA conversion with H-BEA (150) is due to improved molecular diffusion in the pores. Besides the $SiO_2/Al_2O_3$ ratio, other zeolite characteristics such as particle size, surface area may as well play a role but were not further investigated as the goal was achieved to obtain high cyclic ester yields. The L-EG yield is further enhanced to 94% by using distilled L-α-HBA (entry 9).

In contrast with enantiopure α-HBA, racemic α-HBA (*rac*-α-HBA) conversion is slower and less selective in forming cyclic esters, in presence of both type of H-BEA catalysts (entry 10 and 11). A statistical mixture of the L,L; D,D- and L,D- diastereomers was achieved (chiral GC analysis: 25.5% L-EG, 25.6% D-EG, 48.9% L,D-EG). Similar low cyclic ester yields were obtained with *rac*-LA (entry 2), but with a higher selectivity to the *meso*-form (yield = 60%) [2]. α-HIBA, having two methyl side groups attached on the α-carbon is an achiral molecule and like α-HBA a C4 (four carbon)-substrate. However, its reactivity is much lower compared to α-HBA. After a 3h reaction in *o*-xylene at 170°C with H-BEA (150), only 13% of the monomer is converted with the formation of 3% of tetramethylglycolide (TMG) (entry 12). Evidence for the difficult formation of TMG is revealed after 16h reaction, as 84% of α-HIBA is converted but only 5% to TMG (entry 13).

**Table S1.** Synthesis of symmetric cyclic esters from α-hydroxyacids

| entry | Monomer | Catalyst ($SiO_2/Al_2O_3$) | Solvent | $T_{oil\ bath}$ (°C) | Time (h) | X[a] (%) | Yield[b] (%) |
|---|---|---|---|---|---|---|---|
| 1[c] | L-LA | H-BEA (25) | toluene | 130 | 3 | 98 | 78 |
| 2 | *rac*-LA | H-BEA (25) | toluene | 130 | 3 | 91 | 55 |
| 3 | GA | H-BEA (25) | toluene | 130 | 3 | 98 | 4 |
| 4 | L-α-HBA | - | toluene | 130 | 3 | 18 | 5 |
| 5 | L-α-HBA | H-BEA (25) | toluene | 130 | 3 | 22 | 5 |
| 6 | L-α-HBA | H-BEA (25) | ethylbenzene | 160 | 3 | 48 | 20 |
| 7 | L-α-HBA | H-BEA (25) | *o*-xylene | 170 | 3 | 96 | 76 |
| 8 | L-α-HBA | H-BEA (150) | *o*-xylene | 170 | 3 | 98 | 88 |
| 9 | L-α-HBA* | H-BEA (150) | *o*-xylene | 170 | 3 | 99 | 94 |
| 10 | *rac*-α-HBA | H-BEA (25) | *o*-xylene | 170 | 3 | 66 | 25 |
| 11 | *rac*-α-HBA | H-BEA (150) | *o*-xylene | 170 | 3 | 86 | 56 |
| 12 | α-HIBA | H-BEA (150) | *o*-xylene | 170 | 3 | 13 | 3 |
| 13 | α-HIBA | H-BEA (150) | *o*-xylene | 170 | 16 | 84 | 5 |

# SUPPORTING INFORMATION

[a]Conversion is calculated based on all α-OH acid species and determined by $^1$H-NMR. [b]Yield cyclic esters. [c]Result also reported in ref. 1 (our lab).

The above-mentioned results already revealed some reactivity differences between the different substrates GA, L-LA, L-α-HBA and α-HIBA in presence of a heterogeneous catalyst. To clarify this, the inherent activity of the four compounds was compared under the same reaction conditions, without adding a catalyst. Blank reactions were performed in toluene at an oil bath temperature of 130°C for GA and LA, and in *o*-xylene at 170°C for L-α-HBA and α-HIBA. Fig. S2 clearly indicates a conversion (and thus reactivity) decline with increasing steric hindrance of the alkyl chains at the α-position of the acids. GA is more reactive than LA, which is more reactive than α-HBA, even with the latter compound being reacted at elevated temperatures. An even lower inherent reactivity was observed with α-HIBA, suggesting slower spontaneous condensations with substrates having substituted α-carbons. One could expect that less reactive substrates undergo slower oligomerizations and thus tend to form smaller products and favoring ring-closure. To verify this, reactions of L-α-HBA and α-HIBA were performed in presence of a soluble acid catalyst (sulphuric acid). Both reactions resulted in full monomer conversion but yielded less than 5% EG and TMG, showing the need of shape-selective catalysts such as zeolite Beta.

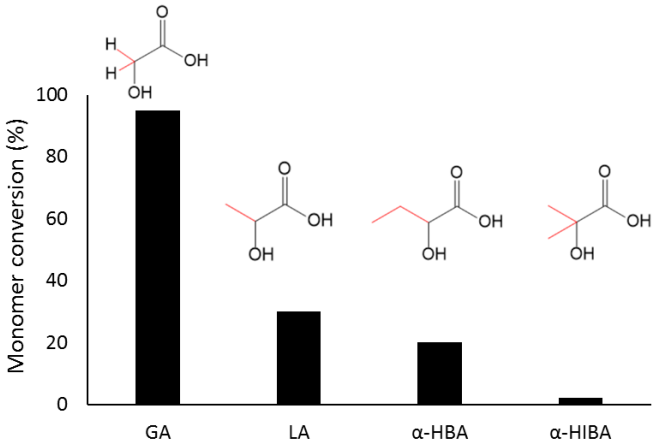


**Fig. S2** Conversion of the different (C2-C4)-α-hydroxy acids. (A) GA and LA: Reaction conditions: 0.5 g monomer, 10 mL toluene, 130°C, 3h. (B) α-HBA and α-HIBA: 0.5 g monomer, 10 mL o-xylene, 170°C, 3h.

Another advantage of the zeolite-based process is the ability to prepare asymmetric cyclic esters in high yields with preferred stereochemistry. Starting from L-LA and L-α-HBA, for example, will result in L-LD, L-EG and the (L,L)- enantiomer of the asymmetric cyclic ester methylethylglycolide (L-MEG). The ability to incorporate both symmetric and asymmetric cyclic esters into lactide co-polymers is very interesting, allowing polymers with a different iteration of side groups having a specific enantioselectivity to be synthesized. Co-polymerization of L-LD with L-EG gives high molecular weight heterotactic polymers with a 2:1 iteration of side groups, whereas switching to the asymmetric L-MEG, one will end up with polymers having a single interruption of ethyl groups.

Co-condensation reactions of L-LA and L-α-HBA were successfully accomplished starting from different monomer ratios, reaching high total cyclic ester yields up to 86% (Table S2). Independent of the monomer ratio of LA:α-HBA, a statistical distribution of cyclic ester products is formed. Hence, if a 90:10 ratio L-LA: L-α-HBA is used, 84% L-LD and 15% L-MEG is formed, along with a negligible amount of L-EG. A 1:1 ratio results in 50% of L-MEG and 25% of each homodimer.

**Table S2.** Synthesis of asymmetric cyclic esters from α-hydroxyacids.

| | | | | | | Distribution (%) | | |
|---|---|---|---|---|---|---|---|---|
| **M1;M2** | **M1:M2** | **Catalyst ($SiO_2/Al_2O_3$)** | **$X_{M1}$ (%)** | **$X_{M2}$ (%)** | **$Y_{CE\ total}$ (%)** | **LD** | **MEG** | **EG** |
| L-LA ; L-α-HBA | 95:5 | H-BEA (25) | 96 | 99 | 83 | 90 | 9 | <1 |
| L-LA ; L-α-HBA | 90:10 | H-BEA (25) | 96 | 99 | 86 | 84 | 15 | <1 |
| L-LA ; D-α-HBA | 50:50 | H-BEA (25) | - | - | 86 | 22 | 42 | 21 |

Diethylglycolide is further purified prior to ring-opening polymerization. After catalytic reaction, the cyclic esters are separated from the linear oligomers and unreacted monomer by toluene-water extraction to obtain an EG purity of 98.0% and an enantiomeric excess (e.e.) of 99.6%. Evaporation of the organic phase was followed by crystallization until a cyclic ester purity of 99.8% (e.e. ≈ 100%) (determined by $^1$H-NMR) was obtained, as a high purity of the monomer and the absence of water in the reaction system are keys to efficaciously obtaining high molecular-weight polyesters. A process flow from feedstock to purified ethylglycolide is displayed in Fig. S3. It was very hard to purify

and isolate pure MEG from the mixed co-condensation reaction products, although this molecule would be highly interesting from a copolymerization point of view.

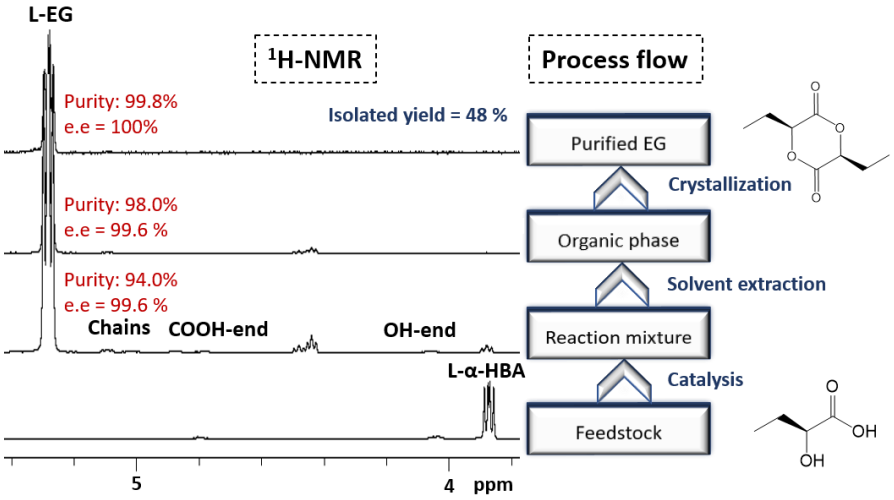


**Fig. S3** Process flow from feedstock (L-α-HBA) to purified ethylglycolide (EG), with the corresponding 1H-NMR spectra (400 MHz, dmso-d6).

## S4 (Co)-polymer synthesis

Diverse co-polymers of L- or D-lactide were synthesized with a small incorporation of L- or D-LD, or L- or D-EG up to 10 mol%. Their chemical structures are depicted in Fig. S4 supplemented with a schematic structure of the polymer backbones.

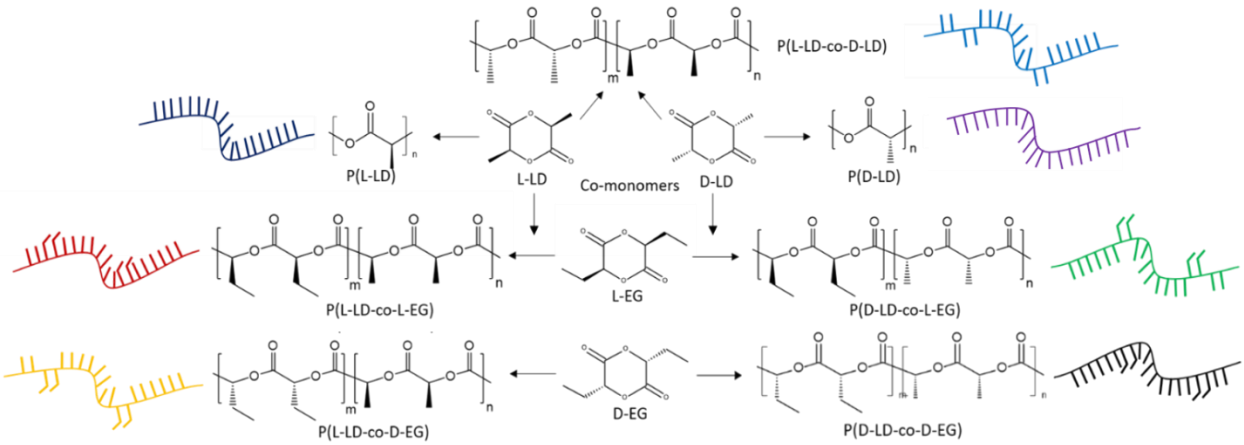


**Fig. S4** Representation of the chemical and schematic structures of all synthesized co-polymers.

The $^{1}$H-NMR spectrum (400MHz, $CDCl_3$) of a co-polymerization reaction of L-LD and L-EG, resulting in a polymer containing 10% L-EG is illustrated in Fig. S5. The figure represents the spectra before and after precipitation of the polymer (L-PLA and L-PEG), dissolved in $CHCl_3$, in methanol to remove residual monomer, catalyst and initiator.

# SUPPORTING INFORMATION

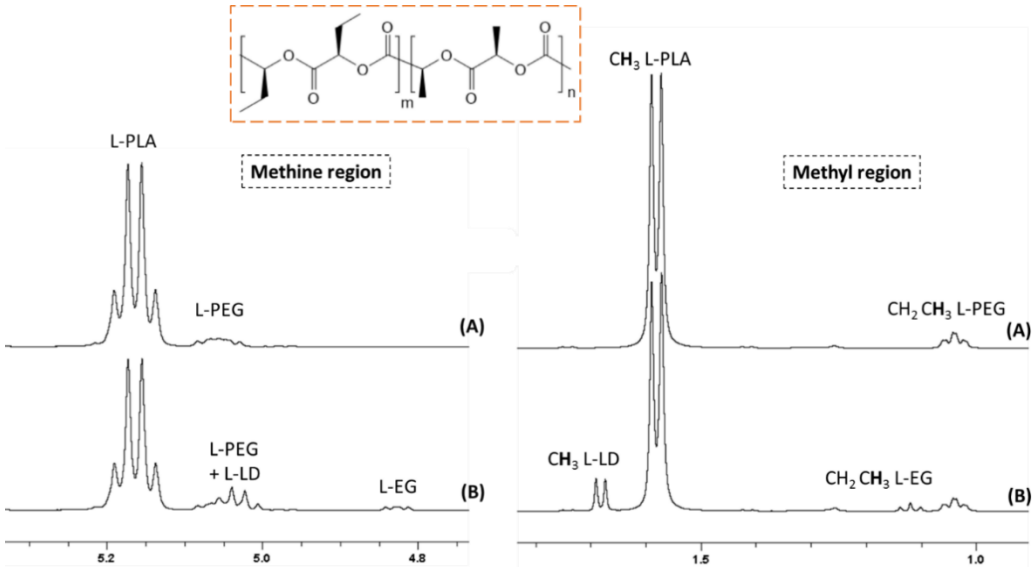


**Fig. S5** $^{1}$H-NMR spectrum (400 MHz, $CDCl_3$) of (A) the polymer after precipitation in methanol (B) of the reaction mixture after ring-opening co-polymerization of L-LD and L-EG. Left = methine protons; Right = methyl protons.

NMR spectra (A) Fig. S5:

**$^{1}$H-NMR** (400 MHz, $CDCl_3$): 5.21-5.11 (1H, q, L-PLA), 5.09-5.01 (1H, m, L-PEG), 2.09-1.87 (2H, m, L-PEG), 1.64- 1.52 (3H, d, L-PLA), 1.09-0.99 (3H, t, L-PEG)

**$^{13}$C-NMR** (600 MHz, $CDCl_3$): 169.6 (L-PLA), 169.1-169.0 (L-PEG), 73.6 (L-PEG), 69.0 (L-PLA), 24.4 (L-PEG), 16.7 (L-PLA), 9.19 (L-PEG)

Table S3 summarizes the results of ROP of LD with various co-monomers. Build-in percentages of the monomers (determined by $^{1}$H-NMR (400 MHz, $CDCl_3$) as well as the weight-average molecular weights ($M_w$, kg mol$^{-1}$) and polydispersity (D) of the polymers are shown. The build-in percentages are average values of the methyl and methine protons, if both were sufficiently visible on $^{1}$H-NMR spectra. The $M_w$ values were determined by GPC analysis with polystyrene standards and corrected by Mark-Houwink's constants for L-PLA [1]. Note that the same Mark-Houwink correction is used as an estimate for all different co-polymers. The $M_w$ values vary between 95.1 and 174 kg/mol and the polydispersity indices lie between 1.3 and 1.9.

# SUPPORTING INFORMATION

**Table S3.** Results of co-polymerization of L(D)-lactide with G, L(D)-lactide or L(D)-EG by ring-opening polymerization

| | | Average build-in % | | GPC | |
|---|---|---|---|---|---|
| **Entry** | **Polymer** | **LD** | **Co-monomer** | **$M_w$ (kg mol$^{-1}$)** | **D** |
| **1** | **P(L-LD) 1** | 100 | / | 144 | 1.5 |
| **2** | **P(L-LD) 2** | 100 | / | 135 | 1.7 |
| **3** | **P(L-LD) 3** | 100 | / | 113 | 1.6 |
| **4** | **P(L-LD) 4** | 100 | / | 112 | 1.6 |
| **5** | **P(L-LD) 5** | 100 | / | 143 | 1.5 |
| **6** | **P(D-LD) 1** | 100 | / | 110 | 1.8 |
| **7** | **P(D-LD) 2** | 100 | / | 117 | 1.7 |
| **8** | **P(L-LD-co-D-LD)** | 90* | 10* | 128 | 1.7 |
| **9** | **P(L-LD-co-L-EG) 1** | 91.0 | 9.0 | 147 | 1.6 |
| **10** | **P(L-LD-co-L-EG) 2** | 94.9 | 5.1 | 95.1 | 1.9 |
| **11** | **P(L-LD-co-L-EG) 3** | 99.3 | 0.7 | 133 | 1.4 |
| **12** | **P(L-LD-co-D-EG) 1** | 89.7 | 10.3 | 101 | 1.4 |
| **13** | **P(L-LD-co-D-EG) 2** | 98.8 | 1.2 | 115 | 1.7 |
| **14** | **P(L-LD-co-D-EG) 3** | 99.9 | 1.1 | 143 | 1.6 |
| **15** | **P(L-LD-co-D-EG) 4** | 99.9 | 1.1 | 110 | 1.7 |
| **16** | **P(L-LD-co-D-EG) 5** | 99.1 | 0.9 | 131 | 1.6 |
| **17** | **P(L-LD-co-D-EG) 6** | 99.3 | 0.7 | 139 | 1.6 |
| **18** | **P(L-LD-co-D-EG) 7** | 99.3 | 0.7 | 174 | 1.4 |
| **19** | **P(L-LD-co-D-EG) 8** | 98.6 | 0.4 | 128 | 1.8 |
| **20** | **P(D-LD-co-D-EG) 1** | 99.4 | 0.6 | 142 | 1.6 |
| **21** | **P(D-LD-co-L-EG) 1** | 89.5 | 10.5 | 131 | 1.7 |
| **22** | **P(D-LD-co-L-EG) 2** | 95.9 | 4.1 | 129 | 1.7 |
| **23** | **P(D-LD-co-L-EG) 3** | 98.0 | 2.0 | 149 | 1.3 |
| **24** | **P(D-LD-co-L-EG) 4** | 98.7 | 1.3 | 147 | 1.4 |
| **25** | **P(D-LD-co-L-EG) 5** | 98.8 | 1.2 | 118 | 1.7 |
| **26** | **P(D-LD-co-L-EG) 6** | 99.2 | 0.8 | 134 | 1.7 |
| **27** | **P(D-LD-co-L-EG) 7** | 99.3 | 0.7 | 128 | 1.5 |
| **28** | **P(D-LD-co-L-EG) 8** | 99.4 | 0.6 | 144 | 1.5 |
| **29** | **P(D-LD-co-L-EG) 9** | 99.7 | 0.3 | 129 | 1.6 |
| **Large scale reactions (50-100g)** | | | | | |
| **30** | **PLLD 6** | 100 | / | 106 | 1.6 |
| **31** | **P(L-LD-co-D-EG) 9** | 98.8 | 1.2 | 119 | 1.9 |
| **Commercial grade PLA (NatureWorks)** | | | | | |
| **32** | **PLA Ingeo 7001D** | 100 | / | 83.3 | 1.5 |

**Added amounts before reaction, difference between L- and D-LD is not visible on $^1$H-NMR*

### *S4.1 Polymerization kinetics*

To determine the possible degree of randomness of the co-polymers the monomer conversions of LD and EG in co-polymerizations were determined over time by $^1$H-NMR (400 MHz, $CDCl_3$). Different samples were taking from a stock solution containing the desired amounts of LD, EG, $Sn(Oct)_2$ (monomer:catalyst = 500-1000:1) and n-dodecanol (initiator:catalyst = 0.7:1) in dry toluene and added to flame-dried vials. Solvent was evaporated under a nitrogen flow and vials were heated at 170°C for different amounts of time (1.5, 3, 5, 10, 15, 30, 45 and 60 min.). Reactions were quenched by immediately cooling the vials in an ice bath after polymerization. The co-monomer ratio (EG:LD) and monomer:catalyst ratio (m:c) were determined via $^1$H-NMR before polymerization (time = 0 min). Monomer conversions are determined by integrating monomer and corresponding polymer signals on $^1$H-NMR for both monomers separately. The data of the experiments can be consulted in Table S4 and Fig. S6.

# SUPPORTING INFORMATION

**Table S4.** Summary of kinetic experiments: co-monomer combination and ratio, and monomer:catalyst ratio (m:c)

| Run | Monomers | mol% EG at time = 0 min ($^1$H-NMR) | m:c ($^1$H-NMR) |
|---|---|---|---|
| 1 | (L,L)-LD + (L,L)-EG | 0.9 | 704 |
| 2 | (L,L)-LD + (L,L)-EG | 1.1 | 909 |
| 3 | (D,D)-LD + (L,L)-EG | 0.5 | 1041 |
| 4 | (D,D)-LD + (L,L)-EG | 1.0 | 489 |

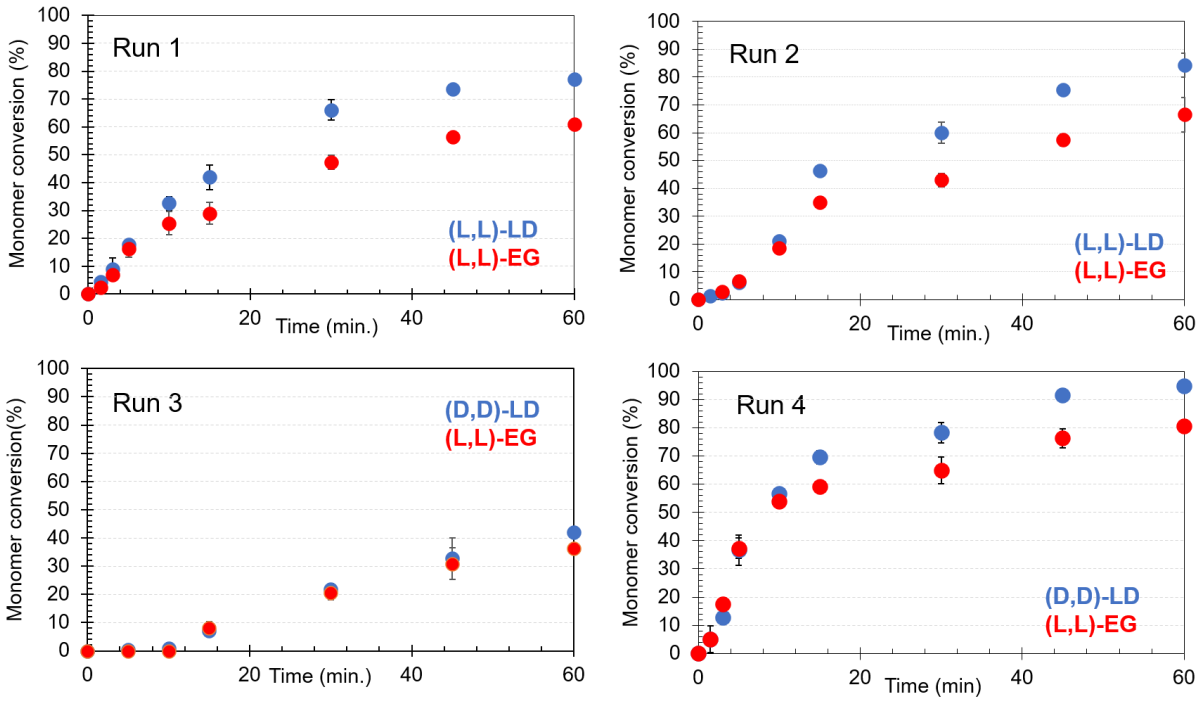


**Fig. S6** Monomer conversion (%) over 60 minutes of ROP of (L,L)-LD and (L,L)-EG or (D,D)-LD and (L,L)-EG for Run 1-4 as described in Table S4.

Although reactions differ slightly in amount of catalyst and co-monomer ratio, it can be clearly seen that the conversions of LD and EG only differ to a small extent at the beginning of polymerization, while near the end of polymerization differences increase.

## S5 Thermal Analysis

Thermal properties of the co-polymers were analyzed by Thermal Gravimetric Analysis (TGA) under both $O_2$ and $N_2$ atmosphere and by Differential Scanning Calorimetry (DSC).

DSC is used to determine the melt temperature ($T_m$, °C), glass transition temperature ($T_g$, °C) and degree of crystallinity ($\chi_c$, %). $T_m$ values are determined from the DSC heating cycles (cycle 1 or 3) and $T_g$ values are determined by analyzing the DSC cooling cycles (cycle 2 or 4). $\chi_c$ is estimated by using the following formula: $\chi_c = \frac{\Delta H_m}{\Delta H_{m,100\%}} \; x \; 100$. $\Delta H_{m,100\%}$ represents the enthalpy of melting for a PLA sample with 100% crystallinity, equal to 93.0 J/g [3]. $\Delta H_m$ represents the enthalpy of melting of the measured sample determined from the heating cycles (cycle 1 or 3). TGA is used to determine the maximum weight-loss rate temperature ($T_{max}$) under both $O_2$ and $N_2$. The data are depicted in Table S5.

# SUPPORTING INFORMATION

**Table S5**. Thermal properties of the co-polymers determined by DSC and TGA

| | | DSC | | | TGA | |
|---|---|---|---|---|---|---|
| **Entry** | **Polymer** | **$T_m$ (°C)** | **$T_g$ (°C)** | **$\chi_c$ (%)** | **$T_{max}$ ($O_2$) (°C)** | **$T_{max}$ ($N_2$) (°C)** |
| **1** | **P(L-LD) 1** | 178 | 55 | 44 | 334 | 293 |
| **2** | **P(L-LD) 2** | 177 | 58 | 46 | 338 | 297 |
| **3** | **P(L-LD) 3** | 179 | 58 | 37 | 340 | 291 |
| **4** | **P(L-LD) 4** | 180 | 58 | 40 | 345 | 318 |
| **5** | **P(L-LD) 5** | 181 | 57 | 42 | 318 | 300 |
| **6** | **P(D-LD) 1** | 180 | 58 | 49 | 297 | 322 |
| **7** | **P(D-LD) 2** | 179 | 567 | 44 | 330 | 330 |
| **8** | **P(L-LD-co-D-LD)** | - | 534 | - | 340 | 323 |
| **9** | **P(L-LD-co-L-EG) 1** | 148 | 43 | 19 | 318 | 311 |
| **10** | **P(L-LD-co-L-EG) 2** | 163 | 48 | 34 | 318 | 297 |
| **11** | **P(L-LD-co-L-EG) 3** | 177 | 54 | 42 | 334 | 320 |
| **12** | **P(L-LD-co-D-EG) 1** | 127 | 46 | **6** | 310 | 298 |
| **13** | **P(L-LD-co-D-EG) 2** | 169 | 56 | 25 | 327 | 299 |
| **14** | **P(L-LD-co-D-EG) 3** | 178 | 58 | 43 | 353 | 313 |
| **15** | **P(L-LD-co-D-EG) 4** | 172 | 57 | 28 | 322 | 297 |
| **16** | **P(L-LD-co-D-EG) 5** | 171 | 57 | 26 | 313 | 301 |
| **17** | **P(L-LD-co-D-EG) 6** | 170 | 54 | 28 | 327 | 310 |
| **18** | **P(L-LD-co-D-EG) 7** | 170 | 59 | 27 | 333 | 309 |
| **19** | **P(L-LD-co-D-EG) 8** | 165 | 57 | 26 | 324 | 304 |
| **20** | **P(D-LD-co-D-EG) 1** | 170 | 56 | 27 | 329 | 321 |
| **21** | **P(D-LD-co-L-EG) 1** | 118 | 45 | 7 | 322 | 316 |
| **22** | **P(D-LD-co-L-EG) 2** | 154 | 55 | 19 | 357 | 291 |
| **23** | **P(D-LD-co-L-EG) 3** | **160** | 57 | 11 | 337 | 323 |
| **24** | **P(D-LD-co-L-EG) 4** | 162 | 58 | 24 | 352 | 308 |
| **25** | **P(D-LD-co-L-EG) 5** | 171 | 56 | 25 | 350 | 309 |
| **26** | **P(D-LD-co-L-EG) 6** | 172 | 59 | 28 | 341 | 314 |
| **27** | **P(D-LD-co-L-EG) 7** | 172 | 59 | 28 | 338 | 298 |
| **28** | **P(D-LD-co-L-EG) 8** | 175 | 58 | 35 | 312 | 303 |
| **29** | **P(D-LD-co-L-EG) 9** | 177 | 56 | 39 | 326 | 304 |
| **Large scale reactions** | | | | | | |
| **30** | **P(L-LD) 6** | 177 | 52 | 34 | 331 | 289 |
| **31** | **P(L-LD-co-D-EG) 9** | 170 | 59 | 29 | 350 | 355 |
| **Commercial grade PLA (NatureWorks)** | | | | | | |
| **32** | **PLA Ingeo 7001D** | 149 | 58 | 1 | 375 | 317 |

Raw DSC and TGA data of a selection of (co-)polymers with high build-in percentage EG are represented in Fig. S7 and Fig. S8 respectively.

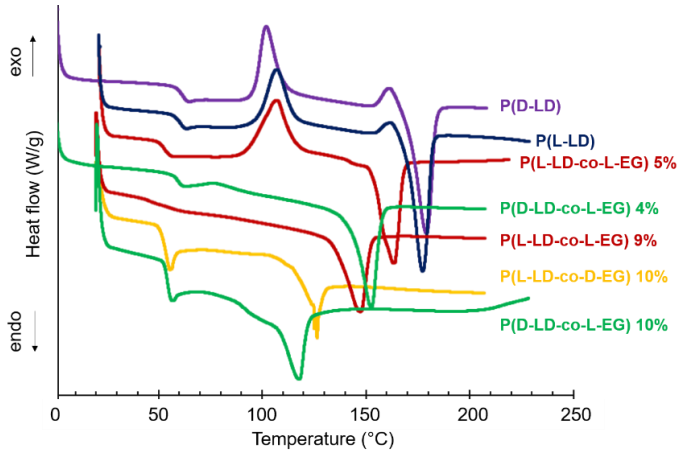


**Fig. S7** DSC data of P(D-LD), P(L-LD), P(L-LD-co-L-EG) 9 and 5% (L-EG), P(D-LD-co-L-EG) 10 and 4% D-EG and P(L-LD-co-D-EG) 10% D-EG.

Fig. S7 clearly shows a decrease in Tm and Tg with addition of EG in P(L-LD) or P(D-LD). P(L-LD-co-L-EG) polymers show a less strong decrease in $T_m$ than P(D-LD-co-L-EG) or P(L-LD-co-D-EG) with a comparable amount of EG co-monomer added to the co-polymers. It can

be seen that crystallinity seems to decrease with addition of EG (witnessed by a decrease in $\Delta H_m$ and a more pronounced glass transition). Crystallinity seems to be stronger affected in co-polymers where LD and EG exhibit opposite chirality.

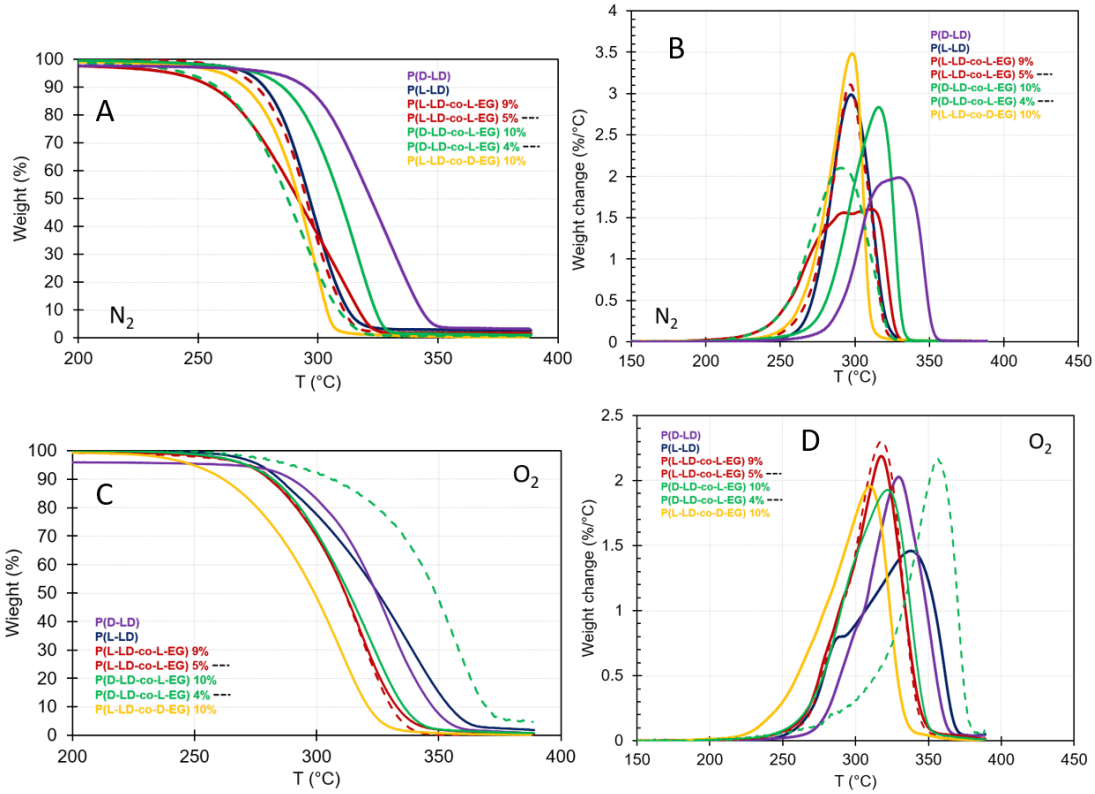


**Fig. S8** Raw TGA data of P(D-LD), P(L-LD), P(L-LD-co-L-EG) 9 and 5% (L-EG), P(D-LD-co-L-EG) 10 and 4% D-EG and P(L-LD-co-D-EG) 10% D-EG measured under N2 ((A) and (B)) and under O2 ((C) and (D)) atmosphere.

Fig. S8 illustrates that differences in thermal degradation behavior between the various co-polymers are rather limited, whereby the temperatures of maximal weight loss ($T_{MAX}$) lays between 289 and 355°C under $N_2$ and between 297 and 353°C under $O_2$. No clear trend is observed for $T_{MAX}$ based on co-polymer composition. According to Yin and Baker [4], the onset of decomposition of substituted polylactides, such as poly(diethylglycolide) shifts to higher temperatures with increasing size of the substituents both under $N_2$ and $O_2$. This is due to the lower volatility of monomers with larger substituents, created during polymer breakdown, and does not necessarily mean a higher stability. This effect is not clearly observed for the synthesized co-polymers and could be due to differences in $M_w$s. One could expect polymers with higher $M_w$s to exhibit a higher thermal stability [5].

## S6 XRD results

X-ray diffractograms of a selection of (co-)polymers are exhibited in Fig. S9. The typical XRD pattern of PLA can be recognized with peaks around 14.9, 16.9, 19.1 and 22.2 degrees.

Addition of EG in high amounts seems to decrease crystallinity (larger amorphous hump) of PLA. This effect seems most pronounced in polymers with opposite chiral nature of LD and EG (P(L-LD-co-D-EG) and P(D-LD-co-L-EG)). No clearly visible new reflections are seen in these diffractograms, indicating the likely absence of other crystal structures.

# SUPPORTING INFORMATION

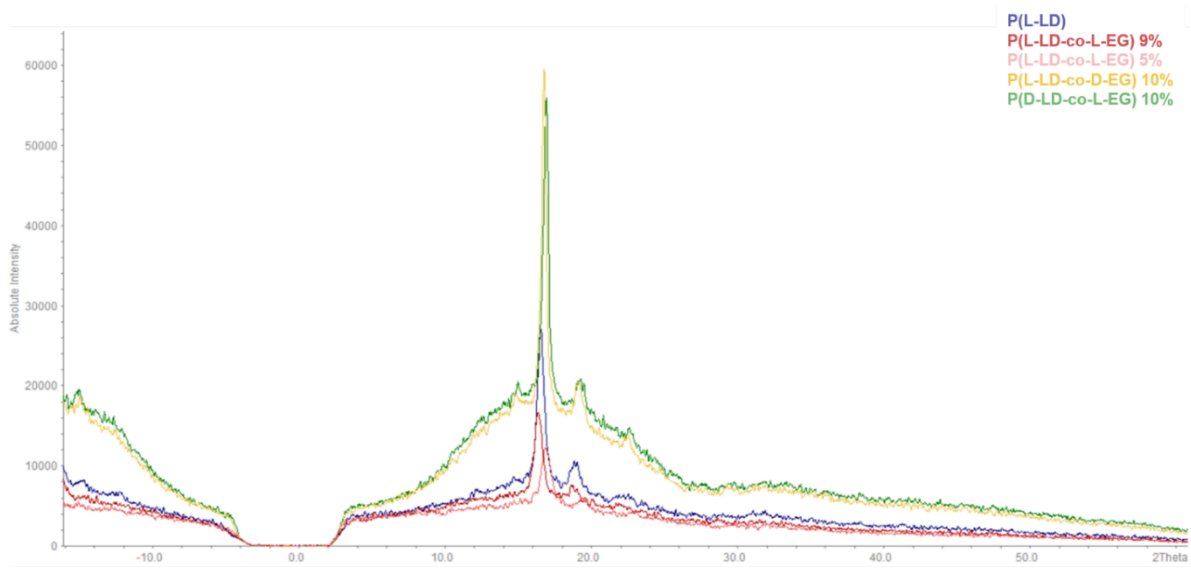


**Fig. S9** XRD results of a selection of (co-)polymers (P(L-LD), P(L-LD-co-L-EG) with 9 and 5% L-EG, P(L-LD-co-D-EG with 10% of D-EG and P(D-LD-co-L-EG) with 10% L-EG).

## S7 Melt Rheology

### *S7.1 Shear rheology*

The flow behavior of the polylactide co-polymers is examined under shear deformation. The viscous and elastic response of the materials under shear strain are studied by strain controlled Small Amplitude Oscillatory Shear (SAOS) rheometry. A small sinusoidal shear strain ($\gamma = \gamma_0 \sin(\omega t)$) is applied on the polyesters and the resultant stress response ($\sigma = \sigma_0 \sin(\omega t + \delta)$) of the material is measured. This measurement determines the modulus of complex viscosity (|η*|), the storage (G') modulus and the loss modulus (G'') as a function of radial frequency (ω) between 0.1 and 100 rad.s$^{-1}$. The oscillation rate at the intersection point of G' and G'' is equal to 1/τ, where τ represents the relaxation time or the time necessary for the material to recover from elastic stress at high ω. The longer the relaxation time and thus the smaller the oscillation rate at cross-over ($\omega_c$), the more elastic the material.

The Carreau-Yasuda model is used to fit the experimental data of the complex viscosity and to determine the zero shear viscosity ($\eta_0$), i.e. the plateau shear viscosity at infinitely low shear rates. The Carreau-Yasuda model is represented by the following equation: $\eta(\dot{\gamma}) = \eta_\infty + (\eta_0 - \eta_\infty)[1 + (\dot{\gamma}\lambda)^a]^{\frac{n-1}{a}}$

Table S6 represents the complex viscosity at 0.1 rad s$^{-1}$, the calculated $\eta_0$ and the ω at cross-over of G' and G'' ($\omega_c$) for all co-polymers.

# SUPPORTING INFORMATION

**Table S6.** Complex viscosity at 0.1 rad.$s^{-1}$, $\eta_0$ and ω at cross-over of G' and G'' ($\omega_c$) determined by SAOS measurements

| Entry | Polymer | \|η*\| (Pa s) at 0.1 rad $s^{-1}$ | $\eta_0$ (Pa s) | $\omega_c$ (rad $s^{-1}$) |
|---|---|---|---|---|
| **1** | **P(L-LD) 1** | 6787 | 7358 | 84.0 |
| **2** | **P(L-LD) 2** | 8806 | 9655 | 62.9 |
| **3** | **P(L-LD) 3** | 1988 | 2082 | > 100 |
| **4** | **P(L-LD) 4** | 18 752 | 20 858 | 45.0 |
| **5** | **P(L-LD) 5** | 22 697 | 25 008 | 36.8 |
| **6** | **P(D-LD) 1** | 13 188 | 14 453 | 62.2 |
| **7** | **P(D-LD) 2** | 11 011 | 12 121 | 84.5 |
| **8** | **P(L-LD-co-D-LD)** | 4730 | 4844 | > 100 |
| **9** | **P(L-LD-co-L-EG) 1** | 7460 | 8343 | 74.8 |
| **10** | **P(L-LD-co-L-EG) 2** | 4956 | 5164 | > 100 |
| **11** | **P(L-LD-co-L-EG) 3** | 18403 | 23 053 | 46.7 |
| **12** | **P(L-LD-co-D-EG) 1** | 14 973 | 15 212 | 80.4 |
| **13** | **P(L-LD-co-D-EG) 2** | 97 424 | 143 302 | 7.83 |
| **14** | **P(L-LD-co-D-EG) 3** | 27 026 | 34 829 | 31.7 |
| **15** | **P(L-LD-co-D-EG) 4** | 59 433 | 87 906 | 14.7 |
| **16** | **P(L-LD-co-D-EG) 5** | 26 155 | 28 684 | 37.2 |
| **17** | **P(L-LD-co-D-EG) 6** | 27 922 | 33 914 | 32.1 |
| **18** | **P(L-LD-co-D-EG) 7** | 57 908 | 83 863 | 16.2 |
| **19** | **P(L-LD-co-D-EG) 8** | 43 341 | 54 834 | 24.3 |
| **20** | **P(D-LD-co-D-EG) 1** | 24 475 | 27 839 | 32.7 |
| **21** | **P(D-LD-co-L-EG) 1** | 56 115 | 71 783 | 19.1 |
| **22** | **P(D-LD-co-L-EG) 2** | 65 615 | 108 235 | 8.17 |
| **23** | **P(D-LD-co-L-EG) 3** | 15 601 | 17 290 | 51.0 |
| **24** | **P(D-LD-co-L-EG) 4** | 27 847 | 33 514 | 29.6 |
| **25** | **P(D-LD-co-L-EG) 5** | 26 844 | 33 310 | 24.3 |
| **26** | **P(D-LD-co-L-EG) 6** | 53 847 | 85 664 | 14.8 |
| **27** | **P(D-LD-co-L-EG) 7** | 119 072 | 191 124 | 6.64 |
| **28** | **P(D-LD-co-L-EG) 8** | 24 934 | 29 137 | 33.2 |
| **29** | **P(D-LD-co-L-EG) 9** | 11 108 | 22 919 | 76.6 |
| **Large scale reactions** | | | | |
| **30** | **P(L-LD) 6** | 6833 | 7060 | > 100 |
| **31** | **P(L-LD-co-D-EG) 9** | 13 894 | 14 750 | 55.9 |
| **Commercial grade PLA (NatureWorks)** | | | | |
| **32** | **PLA Ingeo 7001 D** | 5173 | 5850 | > 100 |
| **Average values P(L-LD) and P(D-LD)** | | | | |
| | **P(L-LD)+P(D-LD)** | 11 258 (stdev = 6786) | 12 324 (stdev = 7585) | > 71.9 |

The raw frequency sweep and rate sweep data of a selection of polymers is represented in Fig. S10.

#### S7.1.1 P(L-LD) and P(D-LD)

SAOS results of all synthesized P(L-LD) and P(D-LD) samples and PLA Ingeo 7001D (NatureWorks) are represented in Fig. S10. Shear viscosity and elasticity of the self-made polymers are comparable, but slightly higher than the values for Ingeo 7001D, most probably due to the lower $M_w$ of the commercial material. The average complex viscosity at 0.1 rad $s^{-1}$ and the average zero shear viscosity of all self-made P(L-LD) and P(D-LD) polymers are calculated to be 11 258 Pa s (standard deviation = 6786 Pa s) and 12 324 Pa s (standard deviation = 7585) for an average $M_w$ of 122.5 kg $mol^{-1}$ (Table S6). The average complex viscosity and error bars are indicated in Fig. S10 A and B.

# SUPPORTING INFORMATION

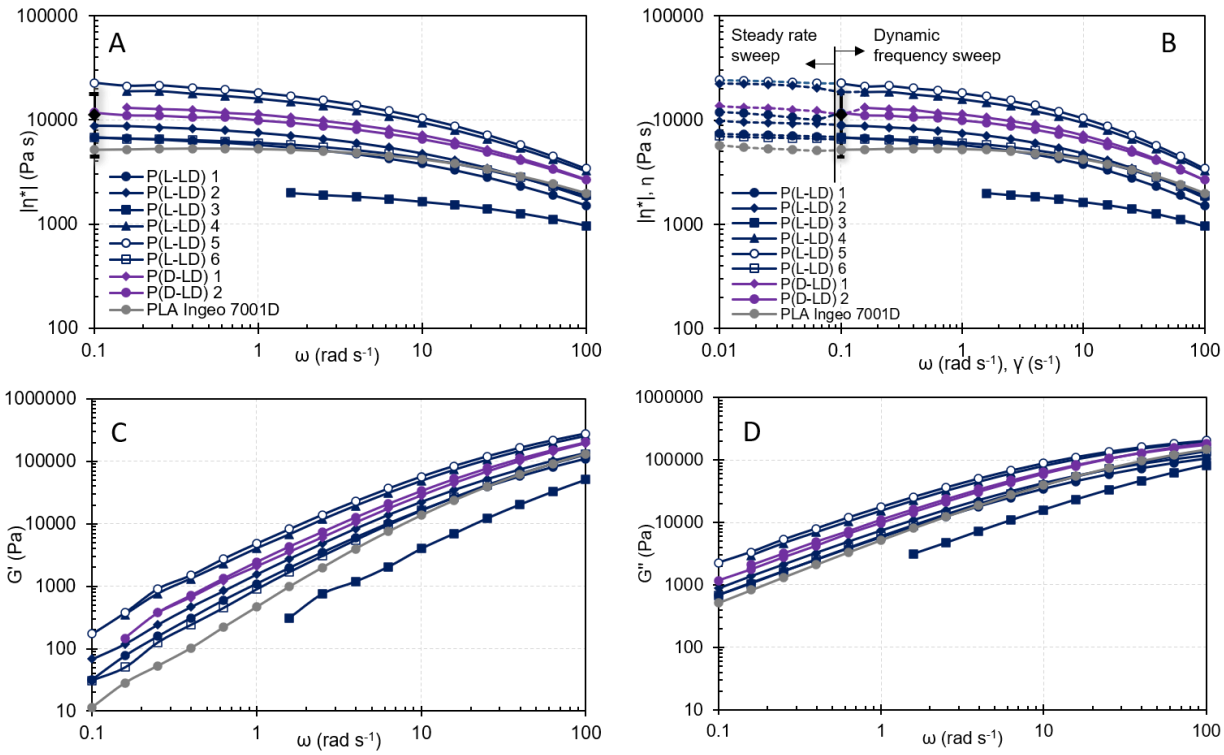


**Fig. S10** (A) complex shear viscosity (|η*|) (dynamic frequency sweep), (B) complex shear viscosity (|η*|) and shear viscosity (η) (steady rate sweep) (C) elastic modulus (G') and (D) viscous modulus (G'') as a function of angular frequency (ω) (or strain rate γ̇) for all synthesized P(L-LD) and P(D-LD) polymers. ◆ and error bars at 0.1 rad.s$^{-1}$ in (A) and (B) indicate the average value and standard deviation of all synthesized P(L-LD)s and P(D-LD)s combined (error bars on y-axis at 0.1 rad s$^{-1}$)

#### S7.1.2 P(L-LD-co-L-EG), P(D-LD-co-D-EG) and P(L-LD-co-D-LD)

Fig. **S11** represents the complex viscosity and G' and G'' data of all synthesized co-polymers containing EG and LD with the same chirality. Data are compared to P(L-LD) 2 (comparable with average value for P(L-LD) and P(D-LD)) and P(L-LD-co-D-LD). A clear improvement in viscosity and elasticity is noticed in P(L-LD-co-L-EG) 3 (0.7% L-EG) and P(D-LD-co-D-EG) 1 (0.6% D-EG), while P(L-LD-co-L-EG) 1 (9% L-EG) and 2 (5% L-EG) exhibit slightly decreased values compared to P(L-LD) 2. Nevertheless, the values of P(L-LD-co-L-EG) 1 and 2 are within the standard variation range of P(L-LD) and P(D-LD), while P(L-LD-co-L-EG) 3 and P(D-LD-co-D-EG) 1 exhibit values a bit above this standard variation range. This might indicate that co-polymers of EG and LD with the same chirality may in certain cases slightly improve viscosity and elasticity but to a limited extend.

# SUPPORTING INFORMATION

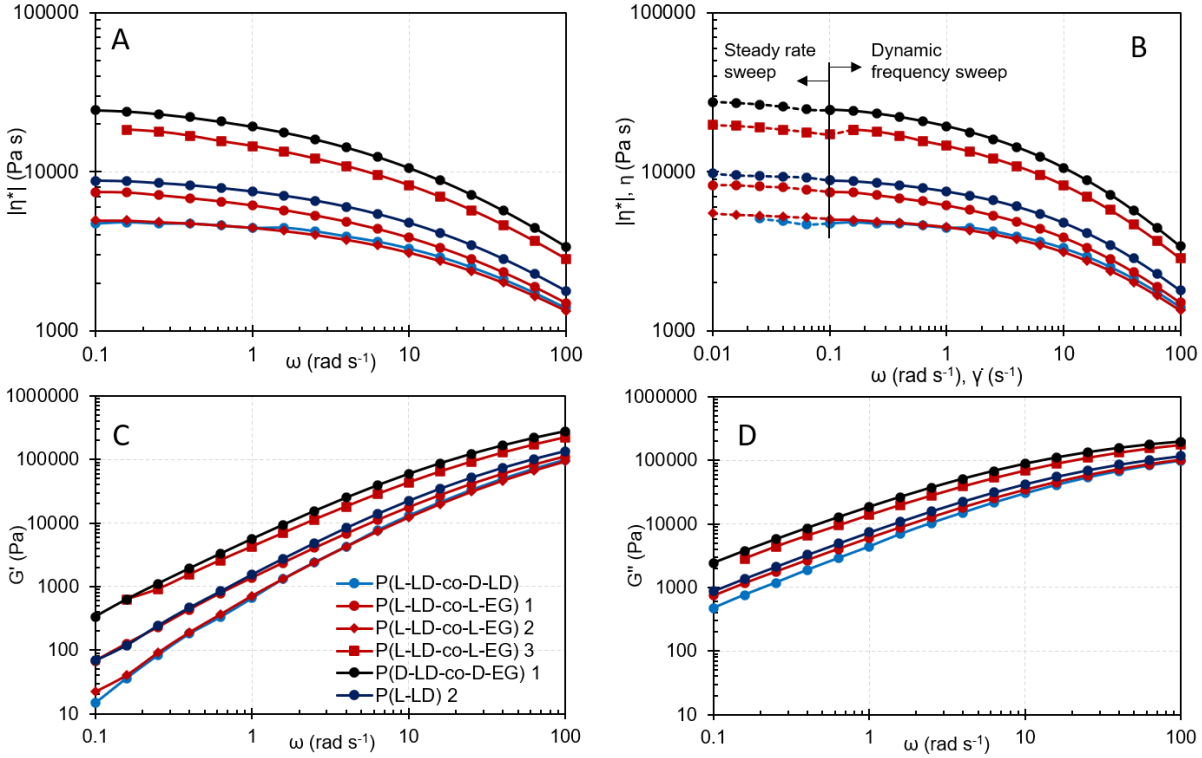


**Fig. S11** (A) complex shear viscosity (|η*|) (dynamic frequency sweep), (B) complex shear viscosity (|η*|) and shear viscosity (η) (steady rate sweep) (C) elastic modulus (G') and (D) viscous modulus (G'') as a function of angular frequency (ω) (or strain rate γ̇) for all synthesized P(L-LD-co-L-EG) and P(D-LD-co-D-EG) co-polymers compared to P(L-LD) 2 and P(L-LD-co-D-LD).

#### S7.1.3 P(L-LD-co-D-EG) and P(D-LD-co-L-EG)

Fig S12 exhibits the G' and G'' values represented on the same graphical plot of a selection of data from Fig. 2 (see paper manuscript) to highlight the visual cross-over of both moduli as a representation of melt elasticity in addition to the $\omega_c$ (rad s-1) values in Table 1 (see paper manuscript).

Fig. **S**3 and Fig. S4 represent the raw complex viscosity and G' and G'' data of a selection of the P(L-LD-co-D-EG) (S13) and P(D-LD-co-L-EG) (S14) co-polymers. Data are compared to P(L-LD) 2 (comparable with average value for P(L-LD) and P(D-LD)).

Fig. S5 shows the $\eta_0$ and $\omega_c$ data of these polymers compared to P(L-LD) 2, P(D-LD) 2 and PLA Ingeo 7001D.

First of all, it can be noticed that all co-polymers exhibit improved shear viscosities and elasticities compared to P(L-LD) 2 (and P(D-LD) 2 and PLA Ingeo 7001D). The values from most co-polymers are observed to be above the standard deviation range of P(L-LD) and P(D-LD), except for P(L-LD-co-D-EG) 1 (10 % D-EG), P(D-LD-co-L-EG) 3 (2% L-EG) and 9 (0.3% L-EG). Some small variations could be attributed to some small differences in $M_w$s. Nevertheless, very strong improvements in melt properties are seen for P(L-LD-co-D-EG) 2 (1.2% D-EG) and 4 (1.0% D-EG) and for P(D-LD-co-L-EG) 1 (10% L-EG), 2 (4% L-EG), 6 (0.8% L-EG) and 7 (0.7% L-EG), which are not attributable to $M_w$s. Although no clear correlation exists between the amount of EG added and the viscosity and elasticity of the materials, these results are reproducible in different samples and strengthen the presumption of a melt-strength improving effect of EG with opposite chirality on poly(lactide).

# SUPPORTING INFORMATION

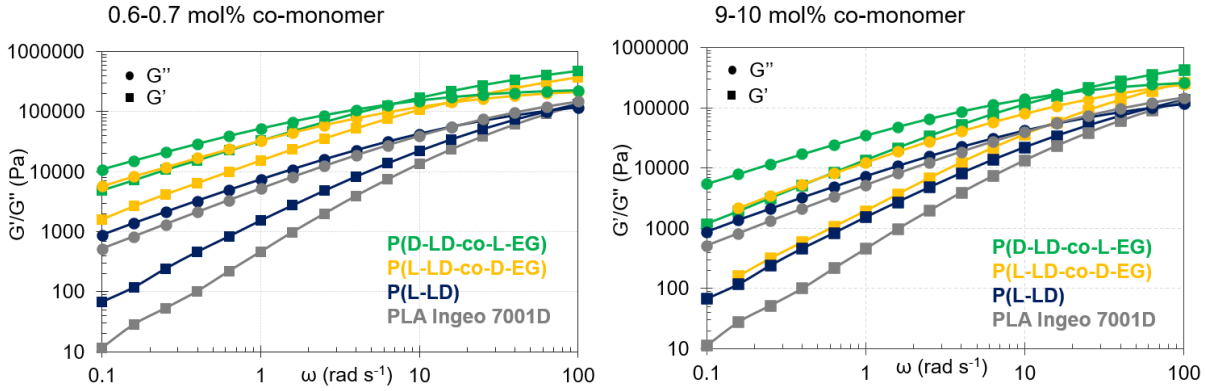


Fig. S12: G' and G'' (Pa) plotted on the same graph for a selection of (co-)polymers with 0.6-0.7mol% and 9-10 mol% of co-monomer

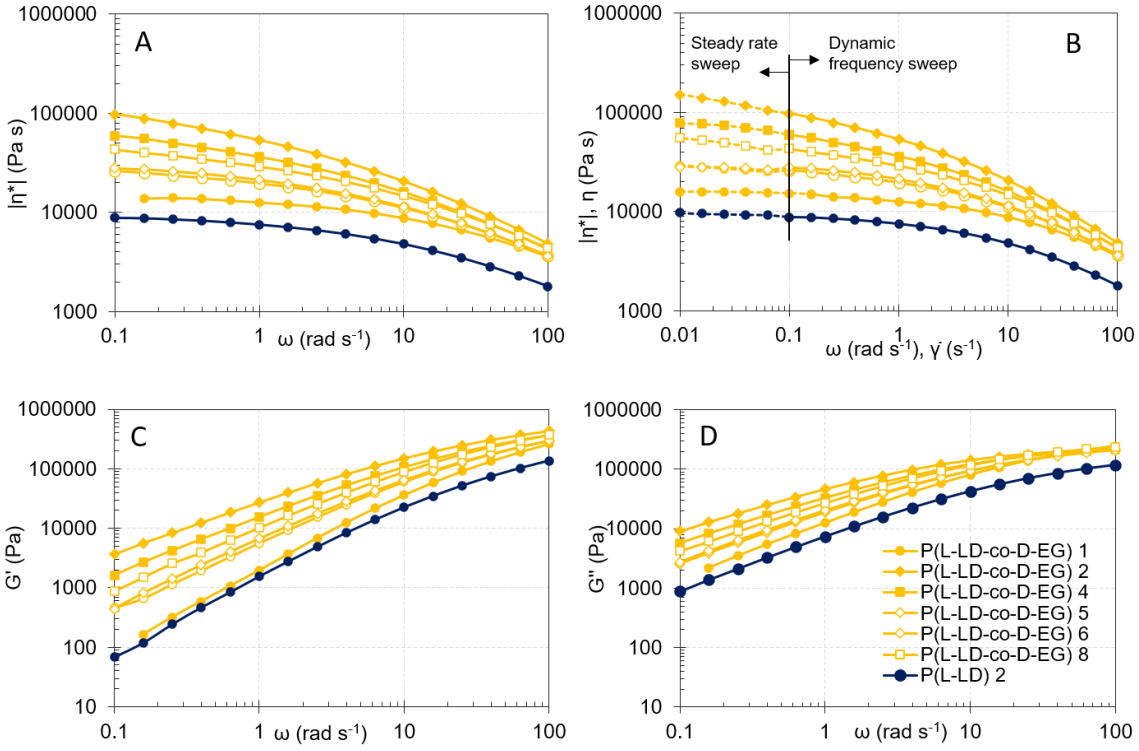


**Fig. S13** (A) complex shear viscosity (|η*|) (dynamic frequency sweep), (B) complex shear viscosity (|η*|) and shear viscosity (η) (steady rate sweep) (C) elastic modulus (G') and (D) viscous modulus (G'') as a function of angular frequency (ω) (or strain rate γ̇) for a selection of the synthesized P(L-LD-co-D-EG) co-polymers compared to P(L-LD) 2.

# SUPPORTING INFORMATION

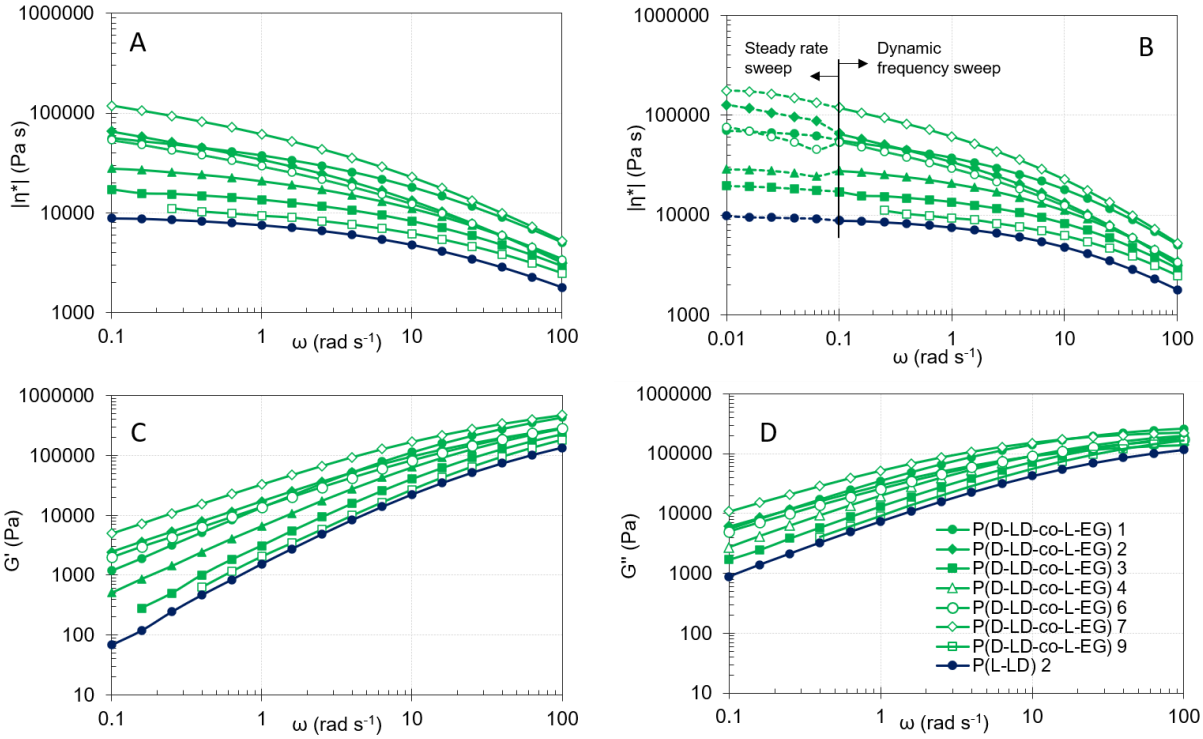


**Fig. S14** (A) complex shear viscosity (|η*|) (dynamic frequency sweep), (B) complex shear viscosity (|η*|) and shear viscosity (η) (steady rate sweep) (C) elastic modulus (G') and (D) viscous modulus (G'') as a function of angular frequency (ω) (or strain rate γ̇) for a selection of the synthesized P(D-LD-co-L-EG) co-polymers compared to P(L-LD) 2.

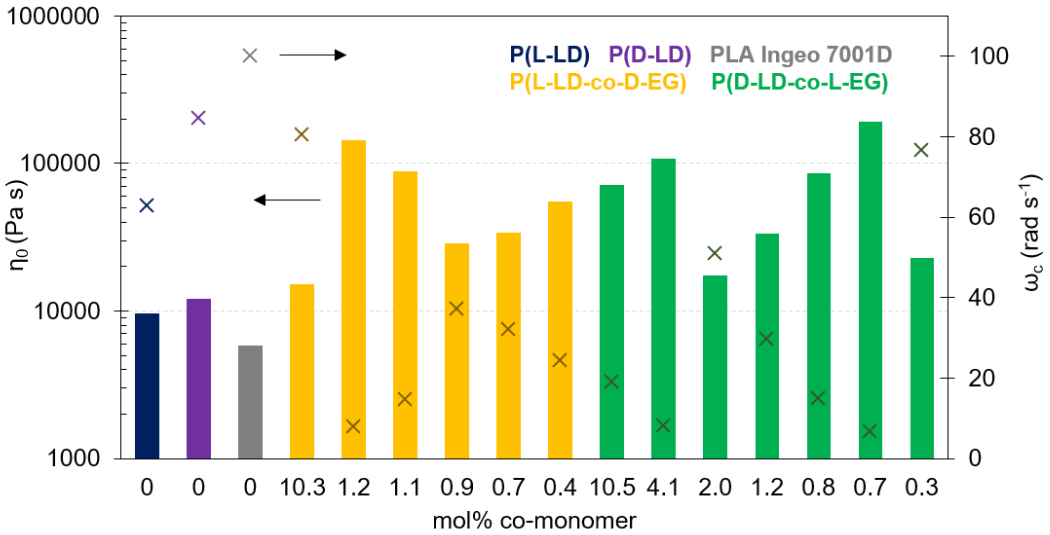


**Fig. S15** Zero shear viscosity $\eta_0$ (Pa s, Carrau Yasuda fitted) (left axis) and angular frequency at cross-over of G' and G'' $\omega_c$ (rad $s^{-1}$) (right axis) of co-polymers of different ratios of co-monomers L-LD and D-EG or D-LD and L-EG compared to references P(L-LD), P(D-LD) and PLA Ingeo 7001D (NatureWorks).

#### S7.1.4 Mark-Houwink correction for differences in Mw

To make sure the viscoelastic effects related to the different co-polymers are not fully attributable to the variations in Mw, a Mark-Houwink correction is applied tot the calculated zero shear viscosities shown in Table 1. For this correction the following formula is used:

$$\eta_0 = \mathrm{K}\, M_w{}^{\alpha} \quad with\ \alpha = 3.4$$

# SUPPORTING INFORMATION

All zero shear viscosity data are corrected toward viscosities at a $M_w$ of 125 kg mol$^{-1}$, being the average Mw of all polymers involved. The corrected zero shear viscosities are depicted in Fig. S16. Note that as an estimate the same value for α is used for all different co-polymers.

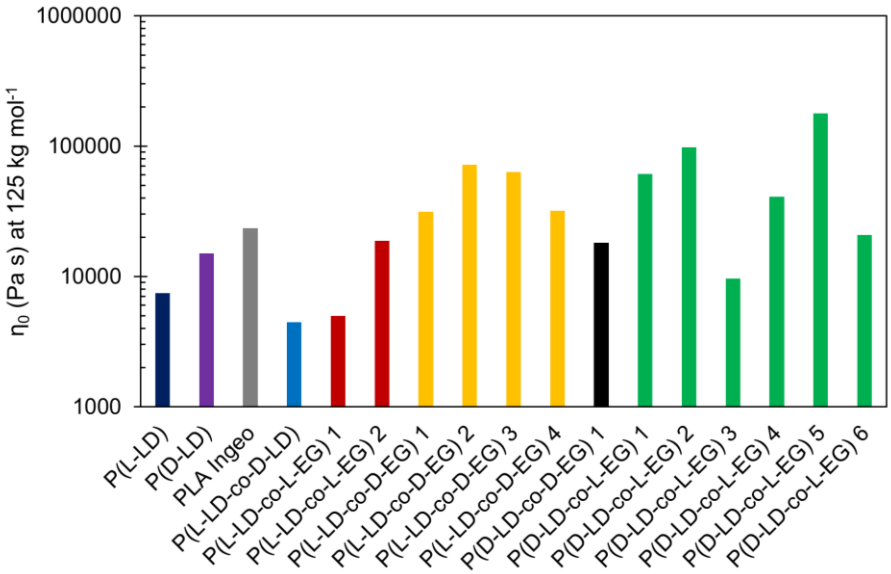


**Fig. S16** Corrected $\eta_0$ values (at 125 kg mol$^{-1}$) of the co-polymers shown in Table 1 for their variations in $M_w$ by means of the Mark-Houwink equation for PLA

#### S7.1.5 Temperature gradient test (shear)

G' and G'' at increasing temperature from 180°C up to 235°C. are measured for P(L-LD)1 and co-polymers of LD and EG with incorporation of about 10 mol% EG. With this test the presence of (stereocomplex) crystalline structures with a melting point above 185°C (till 235°C) (normal measurement temperature) could be detected. If shear viscosities are influenced by these crystallites, one would expect a sudden decrease in shear viscosity and elasticity when their melting point is surpassed. As can be seen in Fig. S17, no sudden decreasing trends are observed within this temperature range, decreasing the likelihood of stereocomplex crystallites within the co-polymer structures.

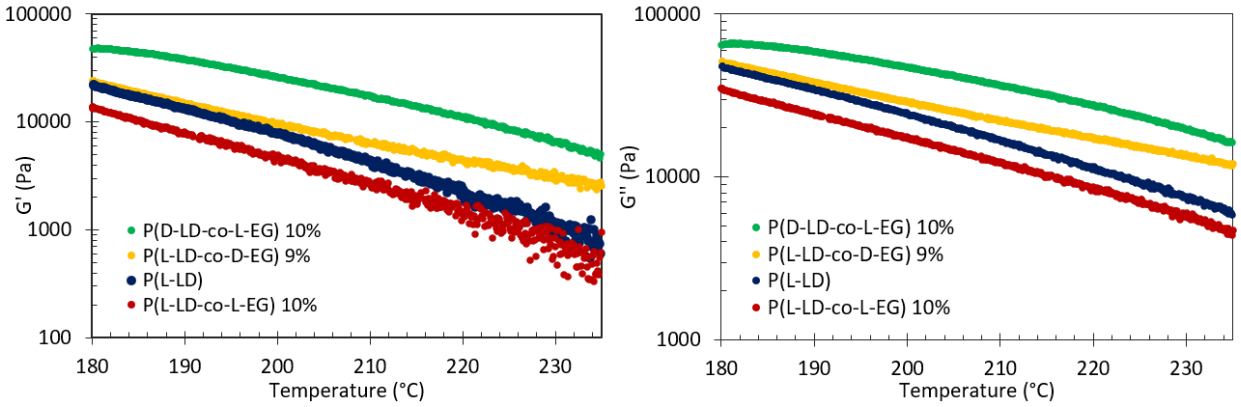


**Fig. S17** G' and G'' at increasing temperature (180°C-230°C) for P(L-LD) 1, P(L-LD-co-L-EG), P(L-LD-co-D-EG) and P(D-LD-co-L-EG) containing 10 mol% of co-monomer.

### *S7.2 Extensional viscosity fixture (EVF)*

To be able to measure polymer melt properties under extensional deformation polymerization reactions were scaled up to 100 g. A polymer of pure L-LD (P(L-LD) 6) and a co-polymer of L-LD and 1.2 mol% D-EG (P(L-LD-co-D-EG 9) were synthesized and their melt properties under extensional deformation were determined by extensional viscosity fixture measurements and compared to a commercial PLA sample (Ingeo 7001D, NatureWorks) designed for injection stretch blow molding applications. Extensional viscosities ($\eta_e$) of the three samples are determined at different Hencky strain rates (0.1, 0.5, 1, 3.5 s$^{-1}$) and compared to each other. Extensional viscosity data are

# SUPPORTING INFORMATION

compared to the shear viscosity data (step rate) at low shear rates (0.05 $s^{-1}$) multiplied by a factor three, as explained by the Trouton ratio ($\eta_e = 3\eta_0$) (see total average data below).

It can be seen that P(L-LD) and PLA Ingeo 7001 exhibit very comparable values, while P(L-LD-co-D-EG) clearly shows higher extensional viscosities (about four times higher).

- ***PLA Ingeo 7001D (NatureWorks)***

***3.5 $s^{-1}$***

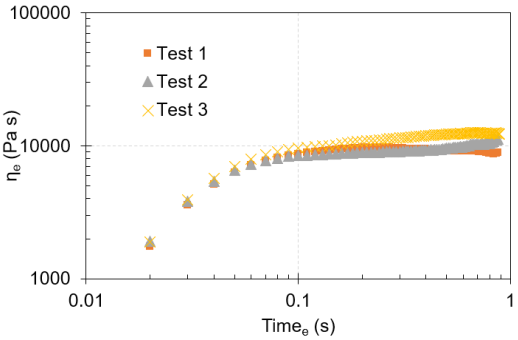


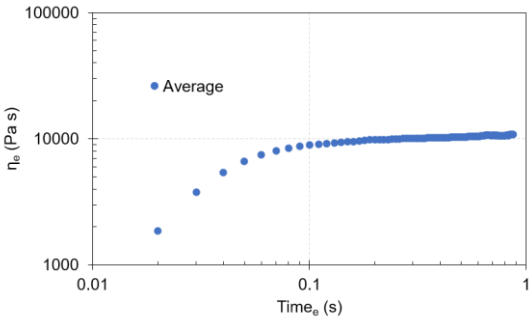


***1 $s^{-1}$***

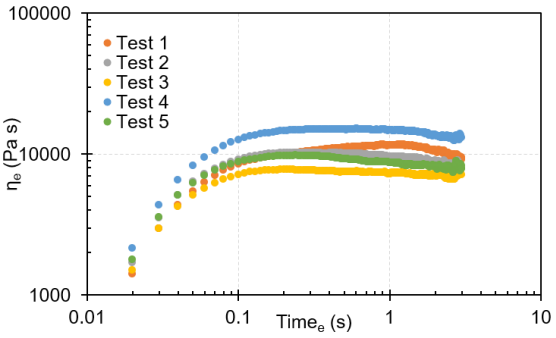


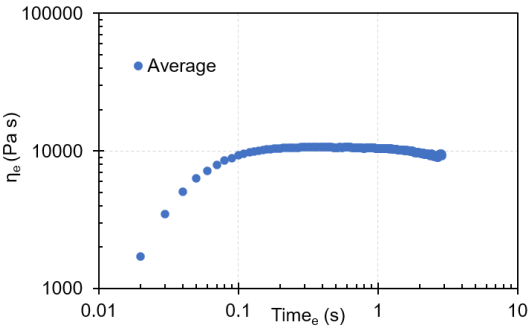


***0.5 $s^{-1}$***

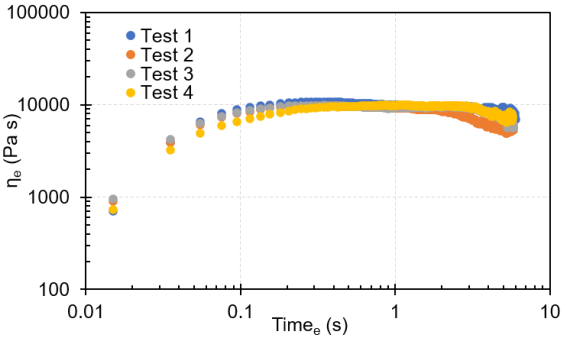


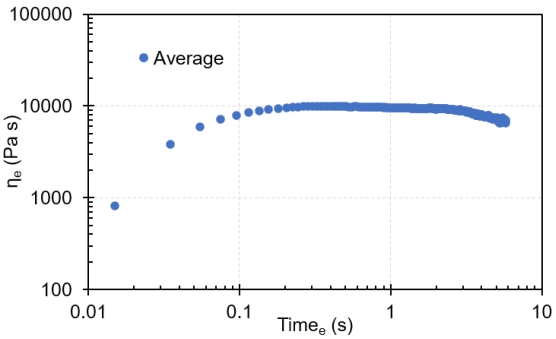

# SUPPORTING INFORMATION

***0.1 $s^{-1}$***

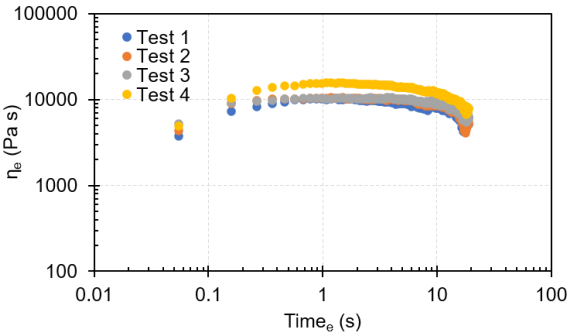


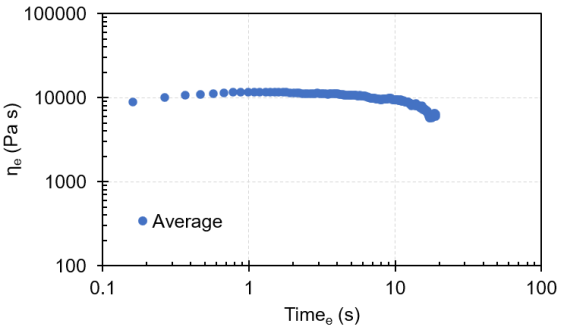


***Total average data***

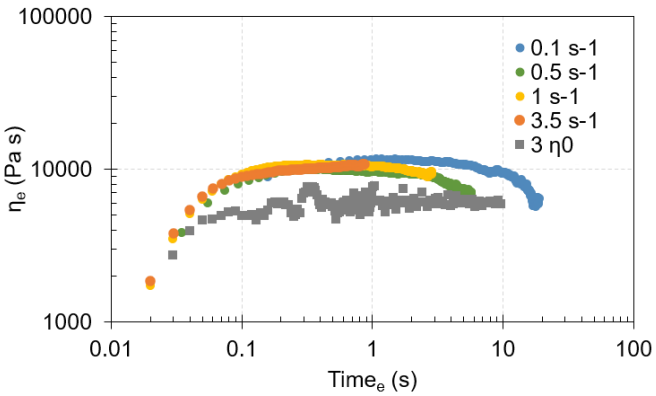


- ***P(L-LD)***

***3.5 $s^{-1}$***

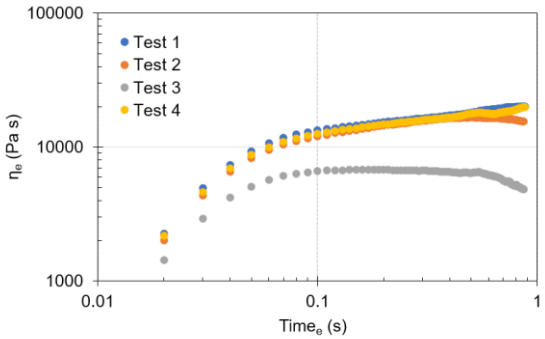


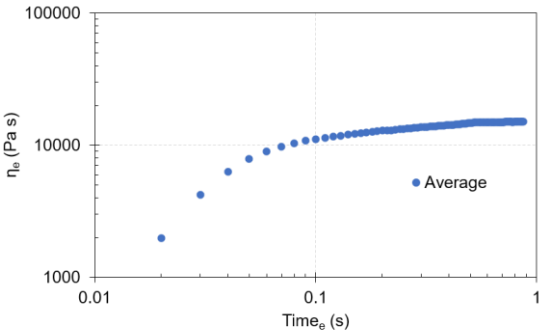

# SUPPORTING INFORMATION

***1 s$^{-1}$***

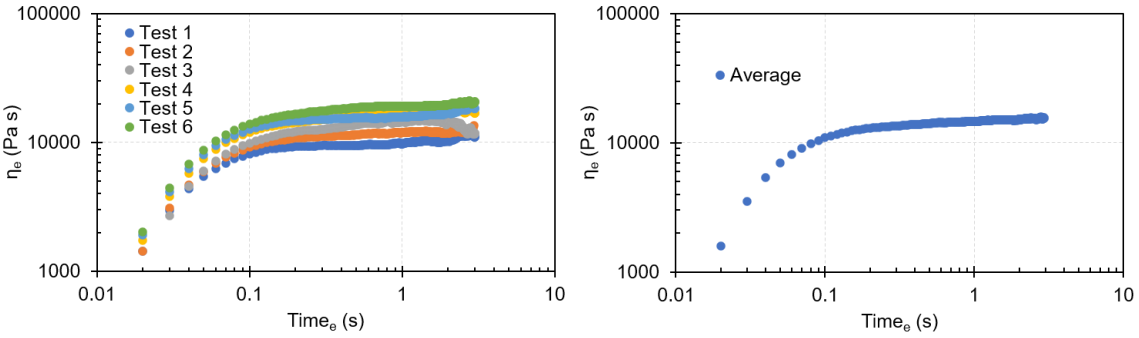


***0.5 s$^{-1}$***

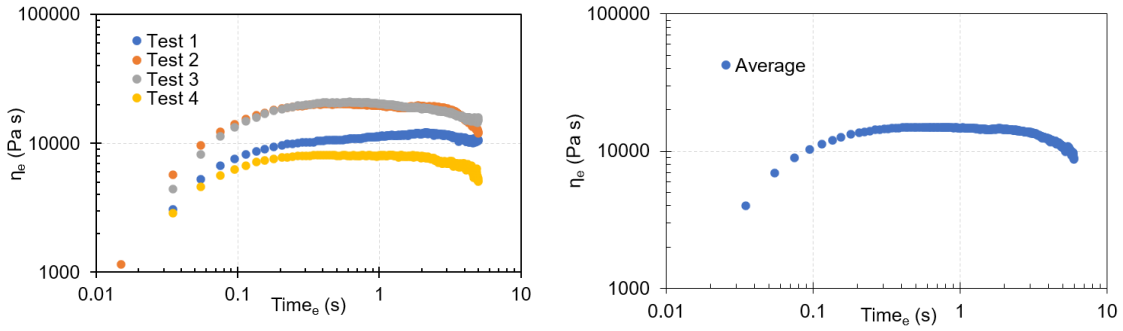


***0.1 s$^{-1}$***

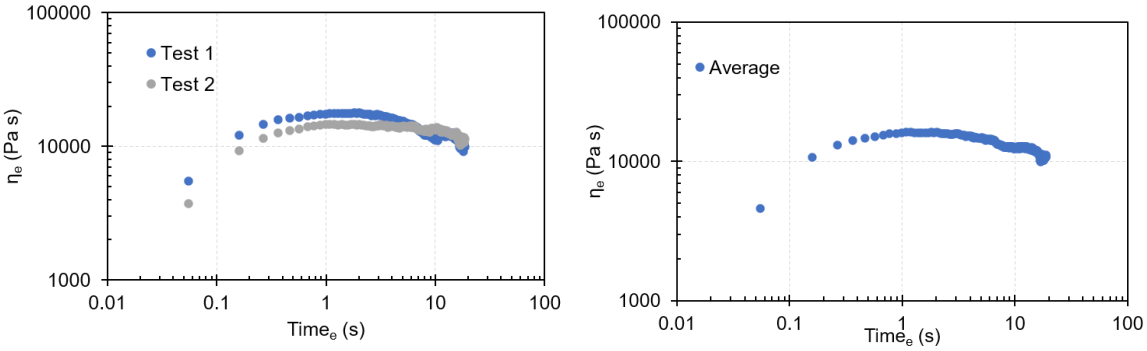

# SUPPORTING INFORMATION

***Total average data***

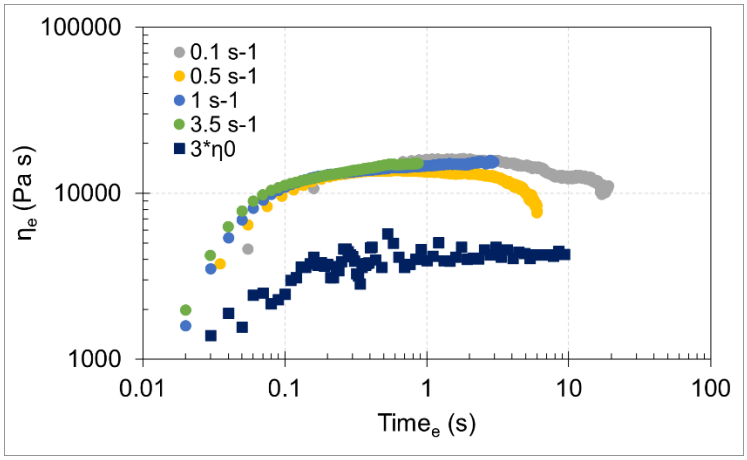


- ***P(L-LD-co-D-EG)***

***3.5 $s^{-1}$***

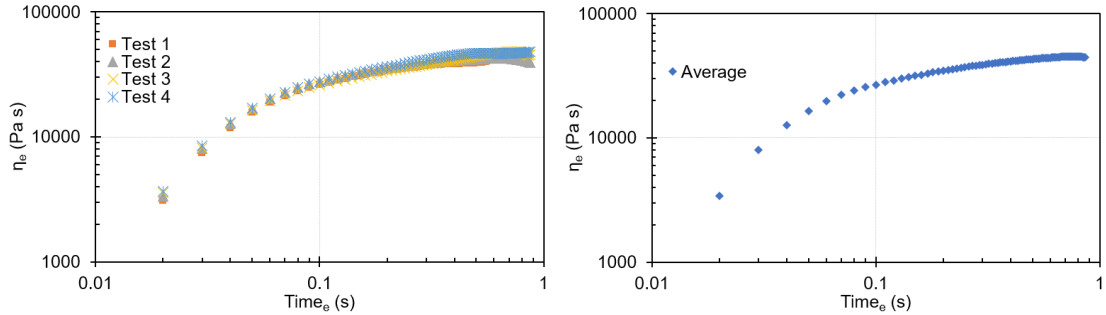


***1 $s^{-1}$***

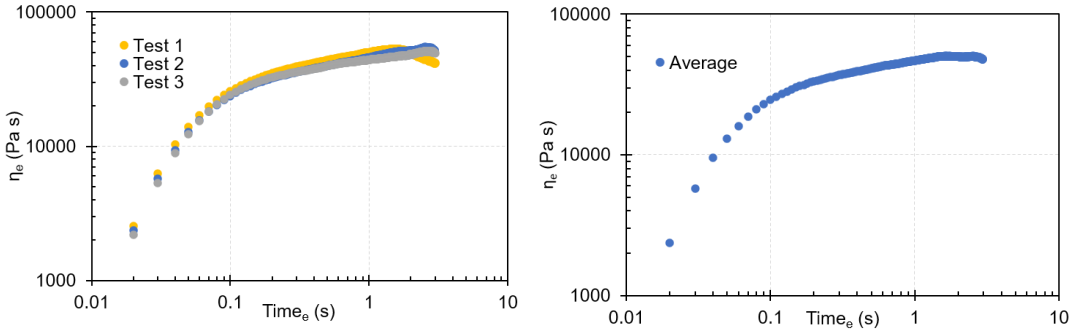

# SUPPORTING INFORMATION

***0.5 $s^{-1}$***

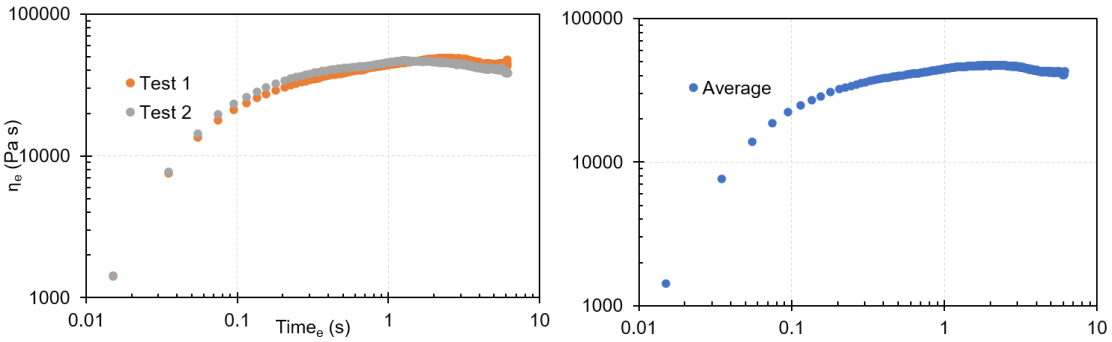


***0.1 $s^{-1}$***

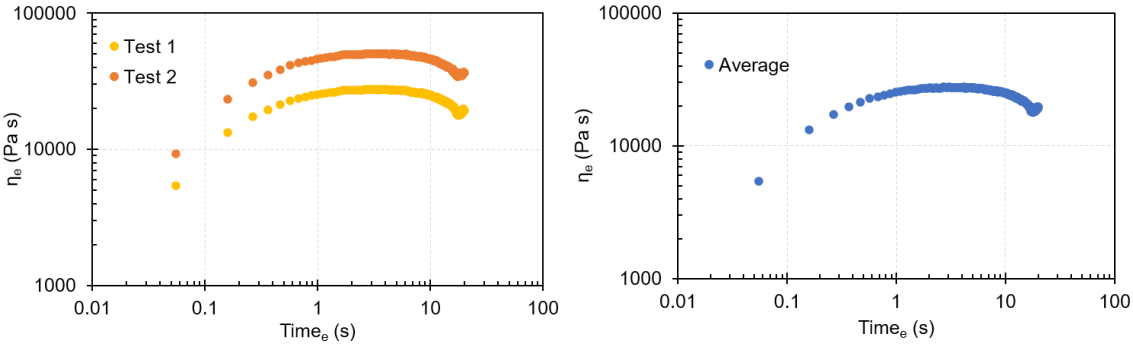


***Total average data***

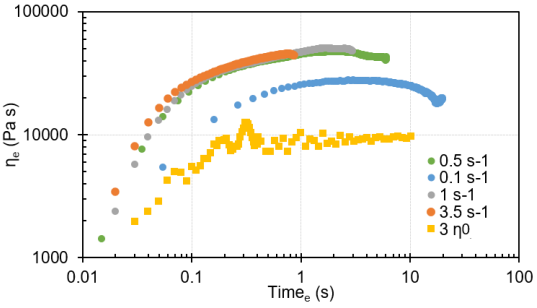


*S7.3 Haul-off*

The raw data from the Haul-off measurements are presented here. Difficulties are observed in obtaining a reproducible speed at which the polymers break (pull-off speed (mm $s^{-1}$). These difficulties can be attributed to vibrations of the Haul-Off apparatus at high rotation speeds and the presence of air bubbles in the polymer melt, which are very difficult to prevent. Nevertheless, extensional forces (N) seem to be reproducible and an interesting difference between the pure polylactides and the synthesized co-polymer is observed. Differences in extensional forces among different measurements for the same polymer samples (P(L-LD) and P(L-LD-co-D-EG)) are attributed to partial thermal degradation and thus losses in $M_w$ due to long-term exposure to high temperatures during the measurements.

# SUPPORTING INFORMATION

**Fig. S18** polymer strands after extrusion of the polymer melt and spinning-up the material on the Haul-off apparatus

- ***PLA Ingeo 7001D***

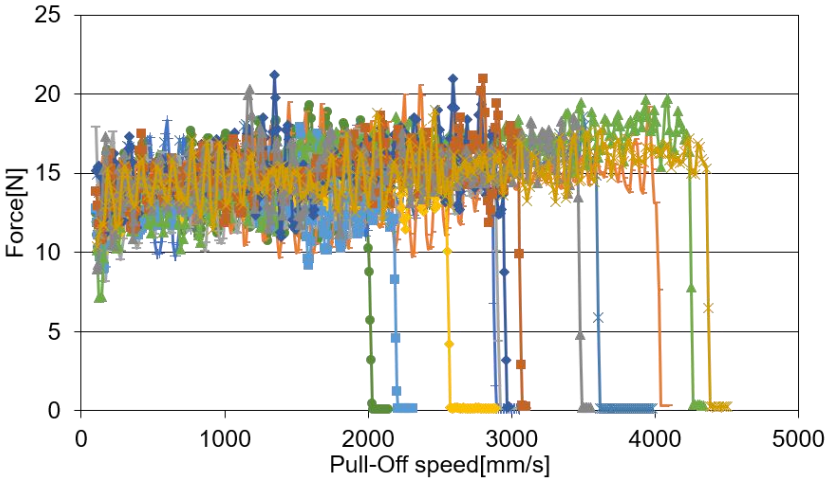


| Measurement | Average Force (N) | Total average Force (N) | Standard deviation (N) |
|---|---|---|---|
| 1 | 15.38182 | 14.54348 | 0.78359 |
| 2 | 14.03966 | | |
| 3 | 14.13436 | | |
| 4 | 14.25072 | | |
| 5 | 13.78011 | | |
| 6 | 13.68419 | | |
| 7 | 13.26847 | | |
| 8 | 15.77031 | | |
| 9 | 15.22303 | | |
| 10 | 15.07627 | | |
| 11 | 14.90230 | | |
| 12 | 15.01058 | | |

# SUPPORTING INFORMATION

- ***P(L-LD)***

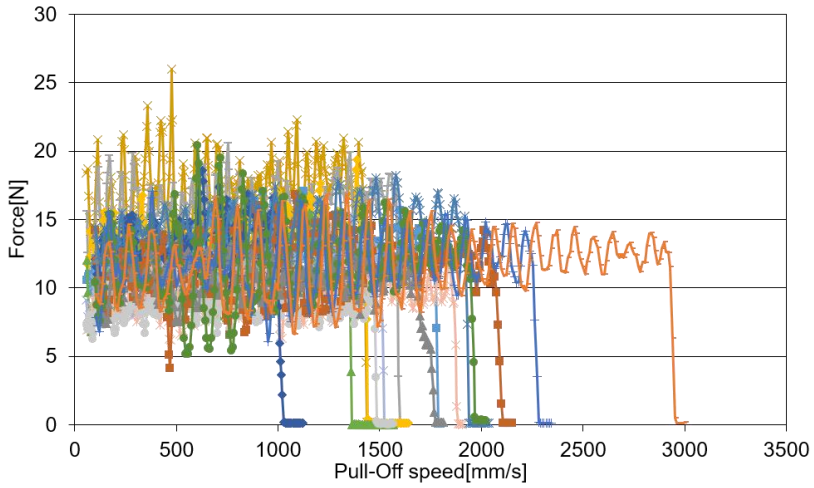


| Measurement | Average Force (N) | Total average Force (N) | Standard deviation (N) |
|---|---|---|---|
| 1 | 13.63368 | 12.41069 | 2.29016 |
| 2 | 11.48173 | | |
| 3 | 10.71977 | | |
| 4 | 14.15122 | | |
| 5 | 14.21869 | | |
| 6 | 11.91466 | | |
| 7 | 11.83858 | | |
| 8 | 11.72567 | | |
| 9 | 17.17812 | | |
| 10 | 15.94848 | | |
| 11 | 13.88767 | | |
| 12 | 12.21825 | | |
| 13 | 10.86880 | | |
| 14 | 10.72457 | | |
| 15 | 9.56915 | | |
| 16 | 8.49202 | | |

- ***P(L-LD-co-D-EG)***

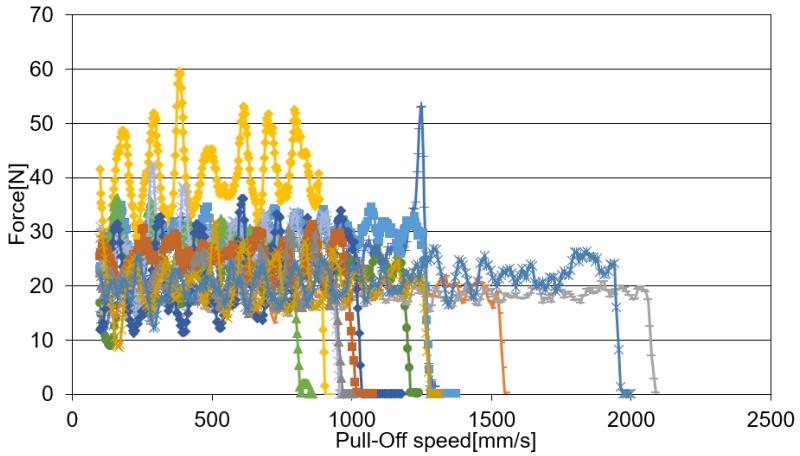

# SUPPORTING INFORMATION

| Measurement | Average Force (N) | Total average Force (N) | Standard deviation (N) |
|---|---|---|---|
| 1 | 20.85069 | 24.40379 | 6.068667 |
| 2 | 24.86096 | | |
| 3 | 18.73099 | | |
| 4 | 17.76959 | | |
| 5 | 40.67158 | | |
| 6 | 29.45681 | | |
| 7 | 27.68893 | | |
| 8 | 27.32110 | | |
| 9 | 21.90033 | | |
| 10 | 25.22833 | | |
| 11 | 21.14445 | | |
| 12 | 20.61324 | | |
| 13 | 21.01227 | | |

# SUPPORTING INFORMATION

## References


[1] D. Garlotta, *J. Polym. Environ.* **2001**, *9*, DOI 10.1023/A:1020200822435.

[2] M. Dusselier, P. Van Wouwe, A. Dewaele, P. A. Jacobs, B. F. Sels, *Science.* **2015**, *349*, 79–81.

[3] D. Battegazzore, S. Bocchini, A. Frache, *eXPRESS Polym. Lett.* **2011**, *5*, 849–858.

[4] M. Yin, G. L. Baker, *Macromolecules* **1999**, *32*, 7711–7718.

[5] F. Carrasco, P. Pagès, J. Gámez-pérez, O. O. Santana, M. L. Maspoch, *Polym. Degrad. Stab.* **2010**, *95*, 116–125.